Newsletters on Stratigraphy, Vol. 52/4 (2019), 461–486
Published online February 25, 2019; published in print September 2019

A comparative study of total organic carbon-$\delta^{13}C$ signatures in the Triassic–Jurassic transitional beds of the Central European Basin and western Tethys shelf seas

Martin Schobben[1, 2]*, Julia Gravendyck[3], Franziska Mangels[1], Ulrich Struck[1, 4], Robert Bussert[5], Wolfram M. Kürschner[6], Dieter Korn[1], P. Martin Sander[7] and Martin Aberhan[1]

With 8 figures and 1 table

Abstract. Stratigraphic studies are an integral component in understanding the chronology of events that led to the end-Triassic mass extinction, by resolving causal relationships between environmental upheavals and biotic response. Successful correlation of Triassic–Jurassic (Tr–J) successions is complicated by the disappearance of macro-fossils that are otherwise central components in stratigraphic studies. This problem is exacerbated in multiple Tr–J sections situated in Europe, where the so-called "Event Beds" – assumed to demarcate the extinction interval – are virtually devoid of fossils. An alternative stratigraphic approach entails the reconstruction of carbon isotope records, where stratigraphic fluctuations in carbon isotope composition are considered to track changes in the global biogeochemical carbon cycle. The predominance of carbonate-lean sections has prompted the reconstruction of total organic carbon (TOC)-based carbon isotope records. However, bulk rock derived TOC is the diagenetically stabilized remnant of organic components that accumulated on the sea floor, and which can originate from multiple sources. In this study, we assess long-term TOC-based carbon isotope trends at two sites: Bonenburg (Central European Basin) and Kuhjoch (the Tr–J Global Stratotype Section and Point; western Tethys shelf seas). We focus on the TOC ^{13}C-enrichment of the Event Beds with the aim of deciphering stratigraphic fluctuations in relation to their main driver (the exogenic carbon pool versus organic matter source changes). By studying the systematic co-variance of several sedimentary parameters (TOC, total nitrogen [TN], and the palynomorph composition), we infer that the TOC composition is possibly characterized by insignificant organic matter source changes in terms of the marine and terrestrial organic carbon contributions. By contrast, a clay mineralogical shift to more K-depleted minerals as well as the elevated occurrence of wood fragments in the Event Beds suggest a terrestrial organic matter source shift from immature substrates to substrates predominated by "pre-aged" or "fossil organic matter" under a changing continental weathering regime. This outcome urges for reservations when

Authors' addresses:
[1] Museum für Naturkunde Berlin, Leibniz-Institut für Evolutions- und Biodiversitätsforschung, Invalidenstr. 43, 10115 Berlin, Germany
[2] Utrecht University, Department of Earth Sciences, Princetonlaan 8A, 3584 CB Utrecht, The Netherlands
[3] Freie Universität Berlin, Institut für Biologie, Altensteinstr. 6, 14195 Berlin, Germany
[4] Freie Universität Berlin, Institut für Geologische Wissenschaften, Malteserstr. 74–100, 12249 Berlin, Germany
[5] Technische Universität Berlin, Institut für Angewandte Geowissenschaften, Ackerstr. 76, 13355 Berlin, Germany
[6] University of Oslo, Departments of Geosciences, P. O. Box 1047 Blindern 0316 Oslo, Norway
[7] University of Bonn, Steinmann Institute, Division of Paleontology, Nussallee 8, 53115 Bonn, Germany
* Corresponding author: m. a. n.schobben@uu.nl

DOI: 10.1127/nos/2019/0499 Gebrüder Borntraeger Science Publishers, Stuttgart, www.borntraeger-cramer.com

interpreting TOC-based carbon isotope records in terms of global C-cycle perturbations, especially when coinciding with lithological and mineralogical changes. On a more positive note, the shift towards positive carbon isotope values appears to be a recurring feature, possibly testifying to a globally significant climate-controlled weathering regime shift.

Key words. carbon cycle, palynostratigraphy, chemostratigraphy, mass extinction, weathering

1. Introduction

The Late Triassic interval is signified by dramatic faunal and floral turnovers on a backdrop of environmental and climatic change (McElwain et al. 1999, Whiteside et al. 2007, Whiteside et al. 2010, van de Schootbrugge et al. 2009, Ruhl et al. 2011, Blumenberg et al. 2016). Contemporaneous intense magmatic activity, known as the Central Atlantic Magmatic Province, has been identified as a potential trigger for these perturbations (e. g., Marzoli et al. 2018). Although being one of the "Big Five" mass extinctions (Raup & Sepkoski 1982), the severity and abruptness of the biodiversity depletion is contested by some authors (e. g., Tanner et al. 2004). Nevertheless, there is evidence of globally elevated latest Triassic extinction rates of benthic organisms (Kiessling et al. 2007), severely disturbed reef ecosystems (Dunhill et al. 2018), selective extinction among hypercalcifying organisms (Hönisch et al. 2012), and a turnover of phytoplankton, marine reptiles, and temnospondyl amphibians (van de Schootbrugge et al. 2007, Wintrich et al. 2017, Konietzko-Meier et al. 2018). These factors altogether rank the event as a pivotal moment in Earth history, which defined the course of evolution and helped shape present-day ecosystems.

Robust stratigraphic frameworks are a necessity to resolve the complex interplay of these environmental changes and consequential biotic responses. Ammonite biozones are used as the official definition for the base of the Jurassic system (von Hillebrandt et al. 2013). Palynostratigraphy is an alternative correlative tool, which has been successfully applied in certain basins (Kuerschner et al. 2007, Bonis et al. 2009). Over the last decades, carbon isotope chemostratigraphy has increasingly gained in importance as the basis for global correlative schemes that link individual Tr–J boundary sections (Palfy et al. 2001, Hesselbo et al. 2002, Guex et al. 2004, Galli et al. 2005, Kuerschner et al. 2007, Ruhl et al. 2009, Bachan et al. 2012, Dal Corso et al. 2014, Yager et al. 2017).

Many studies have focused on pronounced negative shifts in the carbon isotope composition of organic matter, postulating a sudden marine productivity collapse, climate-driven methane hydrate dissociation and volcanism-derived CO_2 as possible triggers for these isotopic signatures (Ward et al. 2001, Palfy et al. 2001, Hesselbo et al. 2002, Whiteside et al. 2010, Ruhl et al. 2011, Dal Corso et al. 2014, Yager et al. 2017). Some authors have also focused on positive carbon isotope excursions observed in sedimentary total organic carbon (TOC) and carbonate rock (Bachan et al. 2012, Yager et al. 2017). The signal-to-noise ratio is low, however, and although compound-specific C isotope analyses confirm a perturbation of the atmosphere–ocean system (Whiteside et al. 2010, Ruhl et al. 2011), noisy records might preclude the faithful recognition of a globally contemporaneous signal (Lindström et al. 2017b). For instance, organic matter source changes might significantly contribute to stratigraphic fluctuations in TOC-based carbon isotope curves and obscure the recognition of signals forced by the exogenic carbon reservoir (Arthur et al. 1985, Popp et al. 1989, van de Schootbrugge et al. 2008). Moreover, high-amplitude sea level fluctuations are a prominent feature of this time interval, which might have caused condensation and sedimentation breaks (Hallam 1981, Hallam & Wignall 1999, Hesselbo et al. 2004), but could also lead to extensive reworking of land-derived sedimentary organic material (Bachan et al. 2012).

A disproportional number of well-studied Tr–J transitional beds are located in Europe (e. g., Jüngst 1928, Morbey 1975, Lund 1977, Karle 1984, Kuerschner et al. 2007, Bonis et al. 2009; 2010, Heunisch et al. 2010, Lindström et al. 2017b, Barth et al. 2018), hence these sites form an excellent basis to test the ubiquity of C isotope signals based on TOC. In addition, correlative schemes based on lithology, macro-fossils and palynomorph assemblages provide an independent stratigraphic framework (von Hillebrandt et al. 2013, Lindström et al. 2017b, Barth et al. 2018).

Many of the European sites exhibit marked lithological changes, with a progradational unit just before the ammonite-defined system boundary that recurs at many localities (Hallam 1981, Hallam & Wignall 1999, Lindström et al. 2017b). Total organic carbon of this lithological unit is accompanied by pronounced higher carbon isotope values in comparison to the bracketing

strata. We deem it necessary to better resolve the organic matter sources of the transitional beds by improving our understanding of the sedimentological and mineralogical characteristics of these lithological units. By not only studying the so-called "Event Beds" (Lindström et al. 2017b) but also the bracketing intervals, placed within a wider geographic context, we try to identify general patterns in the stratigraphic record of the TOC-based C isotopes and to separate the effects of variations in local organic matter sources and global contributions of the exogenic carbon pool.

2. Geological setting

2.1. Palaeogeography of the Central European Basin and the western Tethys shelf seas

During the Late Triassic the area that comprises the modern contours of Europe was situated at temperate latitudes (between 30° N and 50° N) and was largely covered by shallow epicontinental seas from which few scattered continental blocks, such as the Rhenish Massif, and Bohemian Massif and the Fennoscandian High emerged (Fig. 1). Important depocenters of these shallow seas were located in the Central European Basin (CEB) and the western Tethyan shelf seas, which appear to have been structurally connected (Bachmann et al. 2008, Barth et al. 2018). Well-studied Tr–J sections of the western Tethyan shelf are mainly known from the intracratonic Kössen and Eiberg basins. One of these sites, the Kuhjoch section, has been assigned as the Global Stratotype Section and Point (GSSP) for the base of the Jurassic System (von Hillebrandt et al. 2013). In NW Europe, relatively larger parts of the Tr–J boundary succession are likely missing or highly condensed (van de Schootbrugge et al. 2008, Lindström et al. 2017b).

2.2. General lithology of the Central European Basin and the western Tethys shelf seas

A Rhaetian transgression induced deposition of shales and deltaic sandstones of the Contorta Beds along the

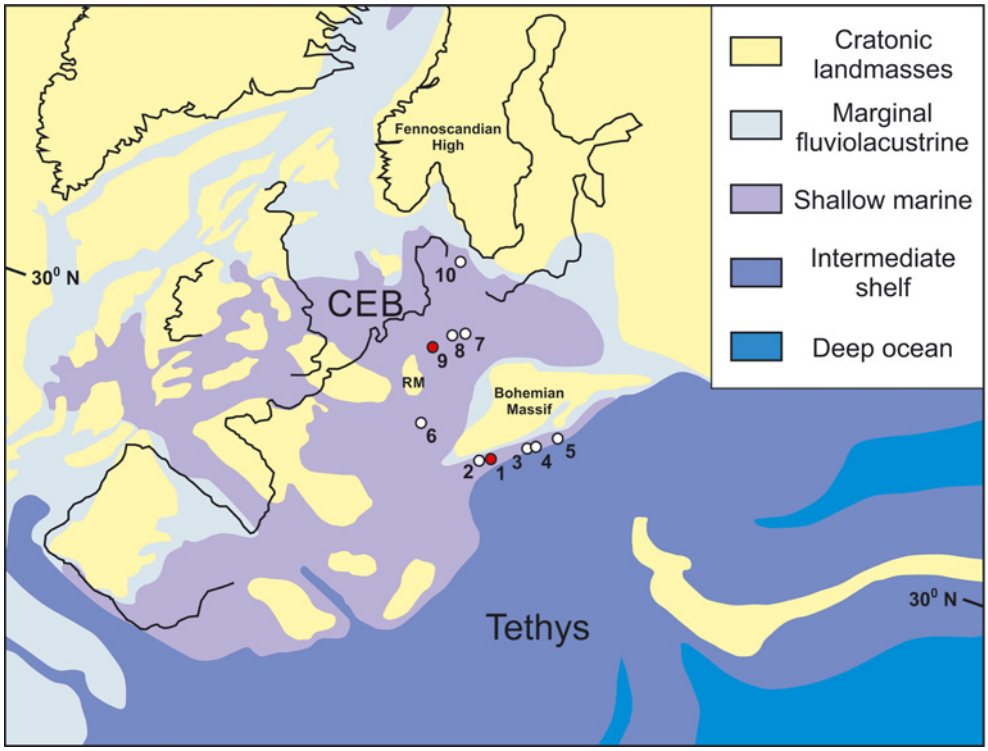

Fig. 1. Geographic reconstruction of the Central European Basin and western Tethys shelf seas in the Late Triassic. 1 – Kuhjoch, 2 – Hochalplgraben, 3 – Kendlbachgraben, 4 – Tiefengraben, 5 – Restentalgraben, 6 – Mingolsheim, 7 – Mariental, 8 – Schandelah, 9 – Bonenburg and 10 – Stenlille (RM = Rhenisch Massif) (modified after: van de Schootbrugge et al. 2009).

north-western half of the CEB, replacing terrestrial lithologies. The Fennoscandian High and the Bohemian Massif are considered the main contributors of detrital sediment input (Nielsen 2003, Bachmann et al. 2008, Fischer et al. 2012, Barth et al. 2018). During the same interval, the western margin of the Tethys Ocean experienced increased siliciclastic sedimentation which reduced the areal extent of previous extensive carbonate platforms (Hauptdolomit Formation/Dachstein Formation) (Hallam 1981, Krystyn et al. 2005, von Hillebrandt et al. 2013). Mixed carbonate and siliciclastic sedimentation (Kössen Formation) continued in intracratonic depressions, such as the Kössen and the Eiberg Basins, which were bordered by reefs at the northern boundary and the southern seaward shelf edge (Oberrhät Limestone). Peak occurrences of marine palynomorphs indicate a Late Triassic sea level highstand in the CEB (Hallam & Wignall 1999, Lindström & Erlström 2007, Barth et al. 2018). In the Eiberg Basin, this interval marks a lithological change, with a distinct dark and bituminous layer, the so-called "T-Bed" (Krystyn et al. 2005, Ruhl et al. 2010).

A subsequent global sea level fall exposed many marine sections around the world (Hallam 1981). However, sedimentation seems uninterrupted in deeper parts of the depocenters, and continued deposition might have been aided by concomitant subsidence (Nielsen 2003, Krystyn et al. 2005, Barth et al. 2018). This change is documented as grey marly deposits of the Tiefengraben Member (Kendlbach Formation) in the Northern Calcareous Alps. In the CEB this drop in sea level has been connected with the formation of a progradational unit of organic matter-poor silt and sandstone, known as the Triletes Beds in Germany and time-equivalent units in Denmark (Lindström et al. 2017b). Another conspicuous and widespread unit in the Eiberg Basin is a bright red clayey marl unit, known as the Schattwald Beds (Lindström et al. 2017b). The similarities of these lithological units of the CEB and western Tethys shelf seas led the previous authors to propose a shared name for these units: the "Event Beds".

A subsequent transgression has been linked with severe condensation and the lack of several earliest Jurassic ammonite biozones in many sections of the CEB (van de Schootbrugge et al. 2008, Lindström et al. 2017b). By contrast, the sections of western Tethys shelf seas document a return to grey marls of the Tiefengraben Member, which contain the oldest known psiloceratid ammonite (*Psiloceras spelae tirolicus*). Eventually, the ongoing transgression resulted in the formation of limestones of the Breitenberg Member (Kendlbach Formation) (von Hillebrandt et al. 2013). Earliest Jurassic sediments of the CEB are generally of an open marine origin with ammonites belonging to the *Planorbis* biozone (Psilonotenton Formation) (e. g., Wetzel 1929, Blind 1963, Bloos 1999, van de Schootbrugge et al. 2009, Lindström et al. 2017b).

3. Materials and Methods

3.1. Materials

The Tr–J transitional beds of the Bonenburg and Kuhjoch sections are studied for their sedimentological, palaeontological, and bulk geochemical characteristics as representatives for the CEB and the western Tethys shelf seas, respectively. The Bonenburg site (51.5631° N; 9.0401° E) is an active brick quarry situated 1 km NW of the village of Bonenburg (City of Warburg, Germany). Samples were taken over a 40 m interval with an approximate resolution of 50 cm. The Kuhjoch GSSP site (47.4839° N; 11.5306° E) is located in the western part of the Northern Calcareous Alps (NCA), 25 km NNE of Innsbruck and 5 km ENE of the village of Hinterriss (Austria). This section (~24 m) was sampled over an interval of 9 m at 20 cm intervals (Bonis et al. 2010, von Hillebrandt et al. 2013). In the lab, the surface of the rock samples was removed to prevent contamination with modern organic material, after which the material was ground manually with agate mortar and pestle, except for a few limestones which were ground with a mechanic agate mill.

3.2. Bulk rock biogeochemical analysis

In order to remove the carbonate content, the samples were treated with 2M HCl and left over night to react at room temperature. This procedure was repeated until no further reaction was observed. The residues were repeatedly washed with MilliQ water^{TM} and dried at 40 °C. The de-carbonated samples were analyzed for total organic carbon content and associated carbon isotopic composition with a THERMOFlash AS 11121 elemental analyzer linked to a THERMO/Finnigan conflo interface (at the Museum für Naturkunde, Berlin). A separate analysis on untreated sample material was carried out to obtain total nitrogen (TN) composition. The analytical precision was mon-

itored by a lab-internal standard (peptone) and yielded relative standard deviations (RSDs) of 3 % for the C and N concentration and 0.05‰ (2SD) for C isotope composition. All carbon isotope measurements are reported in standard delta notation relative to VPDB. Obtained TOC values of de-carbonated substrates were corrected for weight-loss during acid digestion. These analyses were complemented with published carbon isotope data of the Mingolsheim core (Quan et al. 2008), Stenlille core (Lindström et al. 2015), Mariental core (van de Schootbrugge et al. 2013), Schandelah core (van de Schootbrugge et al. 2019) and several outcrops of the NCA (Kuhjoch, Restentalgraben, Kendlbachgraben, Hochalplgraben, and Tiefengraben) (Kuerschner et al. 2007, Ruhl et al. 2009). In addition, TOC, TN and percent carbonate mineral data for Kuhjoch were taken from Ruhl et al. (2010).

Whole rock element analyses have been performed at the Museum für Naturkunde Berlin with a Bruker AXS S8 TIGER on fused samples for major elements. The production of the fused pellets required 0.6 g of ground sample, which had been dried at 105 °C, mixed with 3.6 g of di-lithiumtetraborate together with 0.5 to 20 g of ammoniumnitrate (where the amount depends on the oxidation grade). Subsequently, fusion of sample pellets was performed with an OXIFLUX burner chain in Pt/AU crucibles. Precision of elemental analysis was monitored by analyzing a range of international standards, and repeated measurement of standard element concentrations yielded RSDs that are better than 5 %. Element data of the Kuhjoch section are taken from Tanner et al. (2016).

3.3. Microfloral analysis

Forty-four samples were collected from the Bonenburg section, 19 from the Contorta Beds and 13 from the Triletes Beds of the Exter Formation, and 12 from the Psilonotenton Formation. Palynological processing was performed according to standard laboratory protocols at the palynological laboratory of the department of Geoscience, University of Oslo, Norway. Between 5 and 15 g dry sediment from each sample were crushed and a Lycopodium tablet (containing 12 542 spores on average) was added. Alternate treatments with HCl and HF were conducted to remove carbonate and silicate minerals, respectively. The residue was washed with water until pH was neutral and sieved with a 15 µm mesh, treated with heavy liquid solution ($ZnCl_2$) to remove the remaining inorganic residue (e. g., pyrite), and sieved again with a 15 µm mesh. The organic residue was mounted on four slides per sample with Entellan®Neu. The slides are stored in the collections of the department of Geosciences at the University of Oslo. About 300 organic particles and 300 terrestrial palynomorphs were counted per sample for palynofacies and quantitative palynological analyses, respectively. The rest of each slide plus an additional slide were screened for rare species separately from the palynomorph count for qualitative analysis. Palynomorphs were classified mainly based on Nilsson (1958), Klaus (1960), Schulz (1962, 1967), Morbey (1975), Schuurman (1976), Lund (1977), and Pedersen & Lund (1980). A list of all identified morphotaxa is given in the supplement. First (FO) and last (LO) occurrences of stratigraphically important taxa were identified. This dataset was extended with data from previous palynological studies on the Kuhjoch section (Bonis et al. 2009, Schobben 2011).

3.4. Data processing, statistics and visualization

Data processing, statistical data treatment and visualization were performed on the open-source platform R (R Core Team 2018), and were aided by the R packages: ggplot2 (Wickham 2009), gridExtra (Auguie 2017), ggtern (Hamilton 2017) and broman (Broman & Broman 2017). The palynomorph assemblage zones, as suggested by qualitative analysis, were verified quantitatively by constrained clustering analysis using the CONISS-function in Tilia (Grimm 2011). The manuscript was written as a R Markdown document, and was aided by the R packages: knitr (Xie 2014, Xie 2015, Xie 2018) and kfigr (Koohafkan 2015). The R Markdown file as well as the biogeochemical and microfloral data are available as an online supplement.

4. Chemical weathering indices

The emphasis of this study lies on the contributions of changing organic matter sources and their control on $\delta^{13}C_{TOC}$ fluctuations. Hence, tracing changes in the terrigenous organic carbon (OC) flux over time is a prime objective, and can be forced by changes in the parent material or differential weathering intensities. The same processes would also steer stratigraphic changes in clay mineral assemblages, as thermody-

namic and kinetic constraints determine the chemical composition of clay minerals formed by the weathering of crystalline rocks at Earth's surface (Nesbitt & Young 1984). In essence, the fundamentals of clay chemical composition can, at least in part, be traced back to the parent material, in which some minerals are susceptible to weathering, such as potash feldspar and plagioclase, whereas others are more resistant to weathering, such as quartz and Ti-bearing oxides. These differences can be traced by the selective removal of soluble elements from the parent material with a classical study of the ratios of elements that are presumed to be soluble and mobile against immobile elements. Immobile elements form hydrolyzates and have a large ionic radius, increasing their tendency to be adsorbed on clay minerals (Buggle et al. 2011). Although processes like authigenic clay mineral formation (potentially aided by bacteria), cation adsorption and sorting effects (Konhauser et al. 2002, Michalopoulos & Aller 2004) can skew these generalized assumptions, first-order trends in these element distributions might still be entrained in the chemistry of marine sedimentary rock. For instance, authigenic clay minerals only compose a small percentage of the total sediment mass in deltaic sediments of the Amazon River (Michalopoulos & Aller 2004). Hence, bulk chemistry of the produced material will primarily be controlled by the sediment source and the weathering intensity. By presenting the molar proportions of Na_2O, K_2O and Al_2O_3 on a ternary coordinate system, we attempt to evaluate changes in the terrestrial clay mineral flux for the Tr–J boundary beds of Kuhjoch and Bonenburg.

5. Results

5.1. Litho- and biostratigraphy Bonenburg

The lithological subdivision and palynological zonation can be used to reconstruct an independent stratigraphic framework, enabling a comparative analysis of the supra-regional significance on facies-dependent $\delta^{13}C_{TOC}$ fluctuations. Biostratigraphic information is derived from macroinvertebrates (ammonites, bivalves, conchostracans) and palynomorphs (Fig. 2). Particularly terrestrial palynomorphs, which make up at least 40 and up to 90 % of the palynomorph samples (Fig. 3), exhibit distinct changes in their relative abundances across the Rhaetian and the Tr–J boundary interval at Bonenburg. In this paper, we only present the palynostratigraphically relevant data and five informal assemblage zones of terrestrial palynomorphs that can be recognised (Fig. 2).

Contorta Beds: Thin-bedded to massive mudstones dominate the Contorta Beds. In the basal part of the unit, mudstones and very fine to fine-grained sandstones form coarsening-upward successions. Beds of heterolithic mudstone and sandstone with trace fossils occur sporadically in the middle and upper part of the unit. Shell pavements of marine bivalves and inarticulate brachiopods, bonebeds, and carbonate concretions are intercalated at irregular intervals (Fig. 2). The mudstones contain pyrite and gypsum throughout, whereas dolomite is largely restricted to the middle and upper part. A shift from dark grey to reddish and brownish sediment colours indicates the contact of the Contorta Beds to the Triletes Beds. Biostratigraphically relevant macroinvertebrates of the Contorta Beds include common occurrences of the Rhaetian bivalve *Rhaetavicula contorta* which is the only macrofossil that can be utilized to correlate the Contorta Beds of the CEB with sequences from the western Tethys (Golebiowski 1990). Two other bivalves, *Protocardia rhaetica* and *Pteromya langportensis*, are shared with coeval Rhaetian deposits of the Penarth Group of Great Britain (Ivimey-Cook et al. 1999, Mander et al. 2008) while *P. rhaetica* is also known from Rhaetian deposits of Winterswijk in the Netherlands (Klompmaker et al. 2010).

The Contorta Beds harbor three bonebeds (Fig. 2), labelled bonebed 1 to 3 (Sander et al. 2016, Wintrich et al. 2017). Bonebed 2, the main bonebed, which is subdivided into two layers, bonebed 2 a and bonebed 2 b, contains a typically Rhaetian vertebrate fauna composed of taxa also known from the Bristol Channel area of SW England (Storrs 1994, Korneisel et al. 2015, Mears et al. 2016, Sander et al. 2016, Wintrich et al. 2017). Stratigraphically informative are the chondrichthyan teeth *Hybodus cloacinus*, *Lissodus minimus*, and *Rhomphaiodon minor* as well as the reptile *Pachystropheus rhaeticus* (Sander et al. 2016, Wintrich et al. 2017). In addition, bonebed 2 has produced numerous isolated plesiosaur vertebrae (Sander et al. 2016, Wintrich et al. 2017) and very large shastasaurid ichthyosaur vertebrae typical of the Rhaetian (Fischer et al. 2014, Lomax et al. 2018). Finally, temnospondyl amphibian remains, including the youngest well-dated non-brachiopoid remains, have been found, suggesting a strong influence of the end-Triassic extinction event on temnospondyl amphibians (Konietzko-Meier et al. 2018). Three metres below bonebed 2, the only known

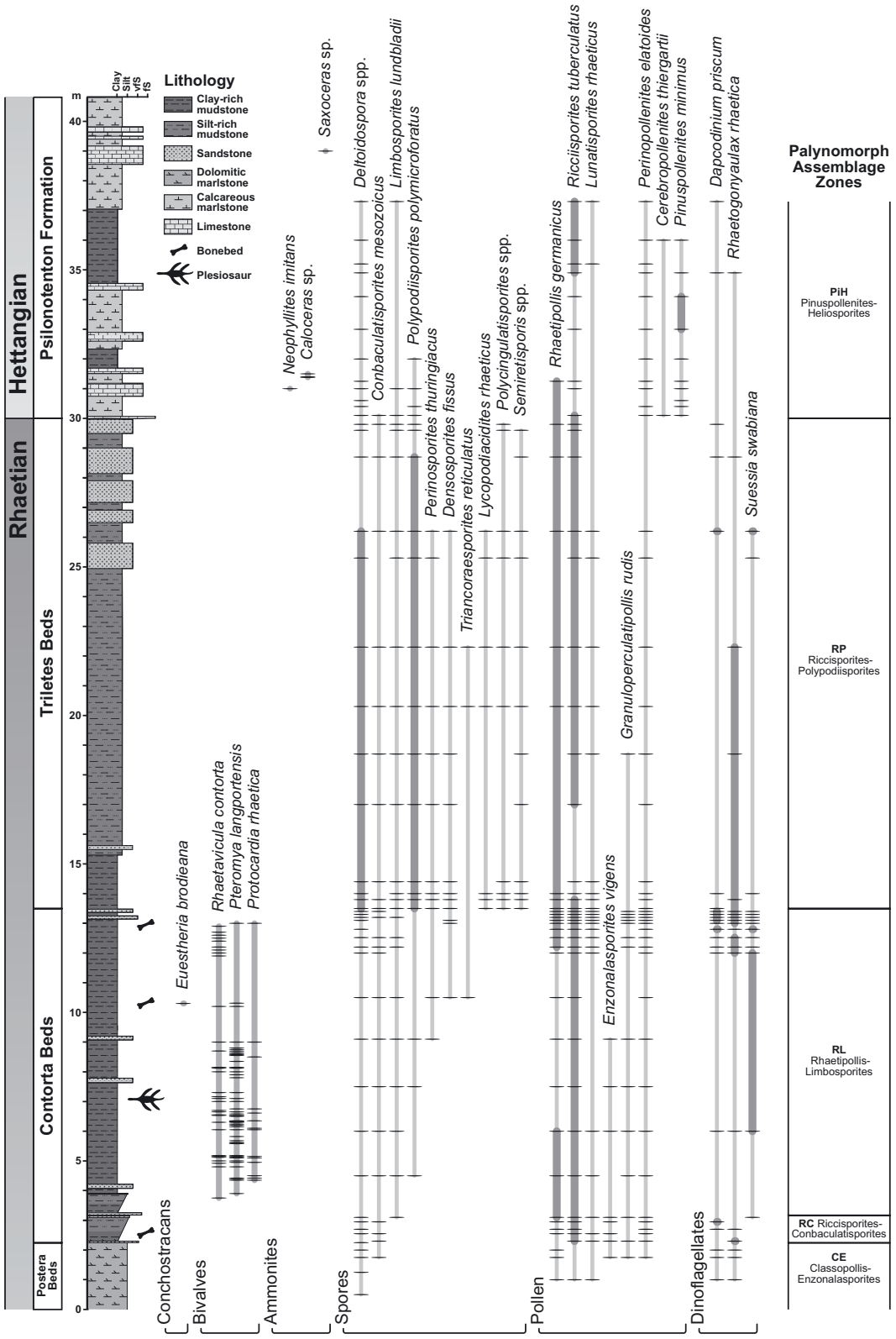

Fig. 2. Lithological column and stratigraphic ranges of key fossils from the Triassic–Jurassic transition at Bonenburg. Horizontal marks indicate the presence of a taxon in a sample. In palynomorph taxon ranges, dark grey segments indicate that the relative abundance of a taxon is higher than 5 % of the terrestrial assemblage (pollen and spores) or the aquatic assemblage (dinoflagellates) respectively. Note variable spacing of analysed samples for invertebrates and palynomorphs.

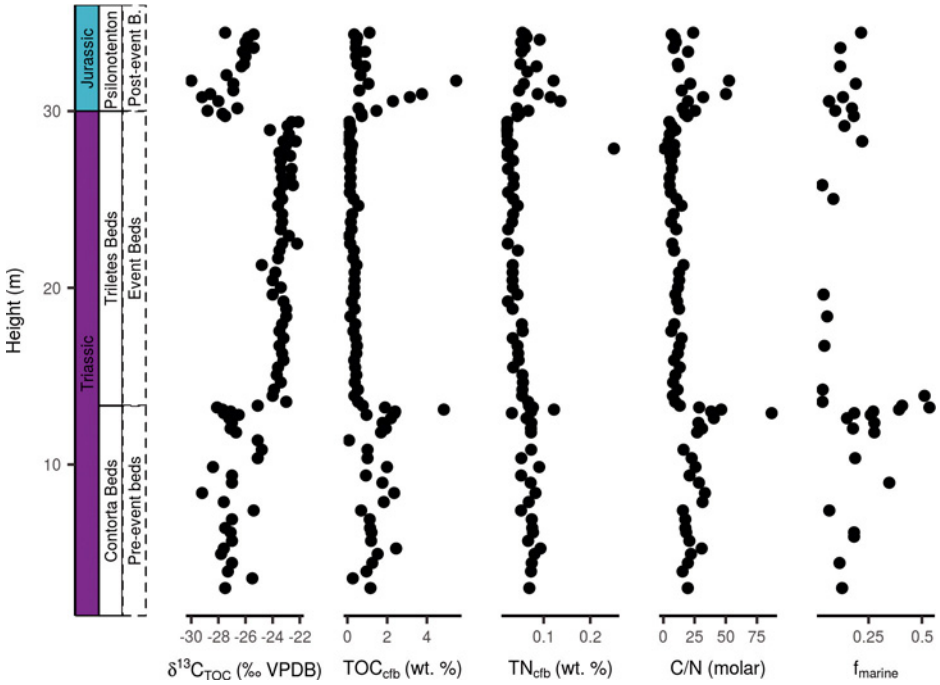

Fig. 3. Stratigraphic plots of total organic carbon-based carbon isotopes, total organic carbon and bulk nitrogen content (cfb stands for carbonate-free basis), molar C to N ratios and the fraction of marine palynomorphs (marine palynomorphs/[marine + terrestrial palynomorphs]) of the Bonenburg section.

Triassic plesiosaur skeleton that unequivocally proves that several lineages of plesiosaurs crossed the Tr–J boundary was recovered (Wintrich et al. 2017).

Immediately below bonebed 2, the chonchostracan *Euestheria brodieana* occurs in several tightly spaced monospecific layers, indicative of the upper Rhaetian *Euestheria brodieana* Zone (Kozur & Weems 2010). Palynologically, the lowermost part of the Contorta Beds (2.2–2.9 m) represents the *Ricciisporites–Conbaculatisporites* Assemblage Zone (RC-Zone; Fig. 2), with the eponymous taxa accompanied by *Classopollis* spp., *Rhaetipollis germanicus* and *Ovalipollis* spp. with the latter three dominating the assemblage. The remainder of the Contorta Beds (2.9–13.5 m) is assigned to the *Rhaetipollis–Limbosporites* Assemblage Zone (RL-Zone; Fig. 2) which is dominated by the eponymous taxa and other pollen such as *Ovalipollis* spp. and *Classopollis* spp. Within the RL-Zone morphotaxa richness increases to 74 taxa because a number of spores – especially the stratigraphically important *Densosporites fissus*, *Perinosporites thuringiacus*, and *Triancoraesporites reticulatus* – have their FOs. Reversely pollen taxa richness decreases and *Granuloperculatisporites rudis* is virtually absent from 9 m up-section with its highest, but only singular, occurrence at 19 m. Of particular stratigraphic importance is the FO of *Limbosporites lundbladii* at the base of this zone.

Triletes Beds (Event Beds): The lower part of the Triletes Beds consists of massive or wavy bedded mudstones and thin sandstones. In the upper part, very fine to fine-grained wavy bedded, ripple cross-bedded and occasionally small-scale cross-bedded sandstones become dominant. Dolomite is present in the lower part of the unit whereas the middle and upper part is calcareous. The biostratigraphic classification of the Triletes Beds is exclusively based on palynomorphs, since macrofossils are absent, except for very few unidentifiable plant remains. The Triletes Beds (13.5–30.0 m) represent the *Ricciisporites–Polypodiisporites* Assemblage Zone (RP-Zone; Fig. 2). With 110 identified taxa, this assemblage zone contains the greatest taxonomic richness and the best preserved palynomorphs within the section. The zone is dominated by spores and characterized by abundant occurrences of *Polypodiisporites polymicroforatus* and *Ricciisporites tuberculatus*. The latter continuously makes up 10–40 % of the terrestrial assemblage while all other pollen, except *Lunatispor-*

ites rhaeticus and *Perinopollenites elatoides*, occur sporadically only. The spore *P. polymicroforatus* makes up 5–20 % of the zone and is joined by a diverse spore assemblage. At the beginning of the last quarter of the Triletes Beds (around 26 m) many palynomorphs have their LOs (e. g., *Densosporites fissus*, *Triancoraesporites reticulatus*, *Perinosporites thuringiacus* and *Lycopodiacidites rhaeticus*), or decline in abundance (*Deltoidospora* spp. and *Concavisporites* spp.). Of biostratigraphic importance is the FO of *Semiretisporis* spp. and *Polycingulatisporites* spp. at the base and their LO at the top of the RP-Zone as well as the LOs of *Densosporites fissus*, *Triancoraesporites reticulatus*, *Perinosporites thuringiacus*, *Lycopodiacidites rhaeticus* at 26 m. Furthermore, palynofacies analyses show a distinct increase in the fraction of wood fragments in this unit.

Psilonotenton Formation: The Triletes Beds are unconformably overlain by an oyster-rich coquinoid limestone bed that belongs to the Psilonotenton Formation. The Tr–J boundary is placed at the base of this erosive oyster shell bed at 30 m, based on ammonoid biostratigraphy and palynoflora (see below). The Psilonotenton Formation consists predominantly of wavy to horizontally bedded marl- and mudstones with only minor limestones and contains marine bivalves and ammonites. The latter allow for a biostratigraphical subdivision of the succession (see discussion for ammonoid zonation and correlations; Section 6.1). Three ammonoid-bearing levels are identified: (1) A single specimen of *Neophyllites imitatum* from the limestone bed at 31 m suggests an attribution of the bed to the second biohorizon of the British standard zonation (Page 2002), indicating the lower part of the *Planorbis* Chronozone. (2) Crushed specimens of *Caloceras* sp. from the limestone bed at 31.5 m indicate a higher position in the *Planorbis* Chronozone (*Johnstoni* Subchronozone). (3) A single specimen of *Saxoceras* sp. from the limestone bed at 39 m allows attribution to the upper part of the *Liassicus* Chronozone (*Laqueus* Subchronozone). This Hettangian part of the section is further characterized palynologically by a dominance of pollen, overall low taxonomic richness and generally poor preservation. *Heliosporites reissingeri* and *Deltoidospora*/*Concavisporites* spp. are the most common spores in this interval. This part of the section is assigned to the *Pinuspollenites-Heliosporites* Assemblage Zone (PiH-Zone; Fig. 2). The previously abundant *Ricciisporites tuberculatus* is substituted by *Classopollis* spp. which markedly increased in abundance from 0–1 % to 36–70 % in the Hettangian part of the section. The lowest part of the PiH-Zone still contains typical elements from the previous zone such as the sporadically occurring *Limbosporites lundbladii* and *Polypodiisporites polymicroforatus*. *Ricciisporites tuberculatus* is still common in the lowermost quantitative Hettangian samples, but strongly decreases in abundance thereafter. The uppermost part of the palynologically studied section is distinguished by the abundant reoccurrence of *Ricciisporites tuberculatus* and scattered occurrences of spores and pollen that were common in the RP Assemblage Zone. Of stratigraphic importance is the FO of *Cerebropollenites thiergartii* and *Pinuspollenites minimus* at the base of the Psilonotenton Formation.

5.2. Litho- and biostratigraphy Kuhjoch

The lithostratigraphy and palynostratigraphy of the Kuhjoch Tr–J GSSP has been intensively studied (e. g., Bonis et al. 2009, von Hillebrandt 2013), and we limit our discussion to the most salient points required to enable a correlation. This correlative scheme differs from the official stratigraphic definitions (Section 2.2 and Fig. 4) in order to test the facies-dependence of the TOC-carbon isotope composition in the Event Beds. The studied interval comprises a ~24 m succession of marine limestone and marl with varying proportions of siliciclastic and carbonate material, and can be decomposed into the following units. 1) **Pre-event Beds**: the topmost 2 m of the Kössen Formation (Eiberg Member), overlain by a dark bituminous layer, with abundant bivalve and fish remains (the so-called "T-Bed"; Krystyn et al. 2005, Ruhl et al. 2010), followed by grey and yellowish-grey marls containing the last occurrences of the ammonoid *Choristoceras marshi* (von Hillebrandt et al. 2013). 2) **Schattwald Beds (Event Beds)**: the lithology changes to a conspicuous bright red-coloured fossil-poor lithology, distinctive for the occurrences of *Polypodiisporites polymicroforatus*, *Ricciisporites tuberculates* and *Deltoidospora* spp. Local tectonics resulted in a minor fault at the top part (2.16 m above the base of this unit), thereby creating a small hiatus. A second outcrop towards the east (Kuhjoch East) of the main site (Kuhjoch West) was excavated, yielding a more gradual transition into the overlying unit. 3) **Post-event Beds**: transition from red to grey marls with thin silt- and sandstone layers more common up-section. At 6.3 m above the top of the Kössen Formation, the

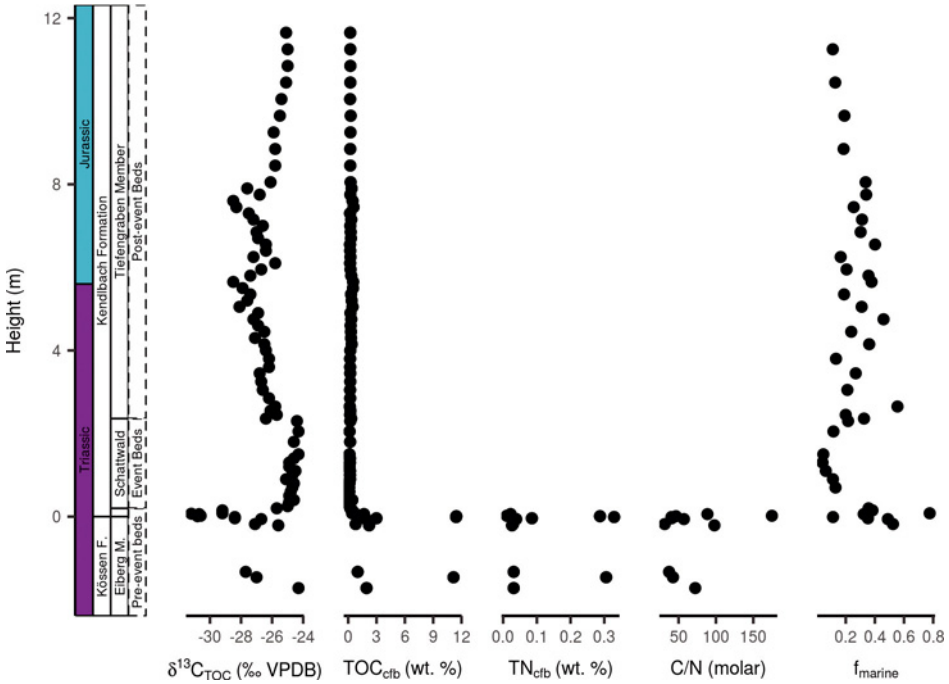

Fig. 4. Stratigraphic plots of total organic carbon-based carbon isotopes, total organic carbon and bulk nitrogen content (cfb stands for carbonate-free basis), molar C to N ratios and the fraction of marine palynomorphs (marine palynomorphs/[marine + terrestrial palynomorphs]) of the Kuhjoch section.

ammonite *Psiloceras spelae tirolicum* appears. The first occurrences of *Cerebropollenites thiergartii* and *Ischyosporites variegatus* are used as informal stratigraphic markers for the Tr–J boundary (von Hillebrandt et al. 2013).

5.3. Comparative mineralogy of the Tr–J transition beds

The Kuhjoch material is relatively more depleted in Na_2O and K_2O content when compared with the Bonenburg sediments, thereby alluding to a different source or local weathering regime (Fig. 5). A shared characteristic of Kuhjoch and Bonenburg is a clear differentiation between the chemical composition of the major lithological units, with the Schattwald and Triletes Beds being the most depleted in K_2O and Na_2O, indicating a higher predominance of K-depleted minerals (e. g., kaolinite) in the mineral assemblage. By contrast, the Hettangian samples of both sites have relatively enriched values of K_2O and Na_2O, indicative of less intense weathering in the source area or a different source of clay mineral production. Most immature are the sediments of the Pre-event Beds of Kuhjoch and the Contorta Beds of Bonenburg. Powder X-ray diffraction of the Bonenburg sediments supplemented by X-ray analyses of <2 μm fractions of selected samples show that the clay mineral assemblage of the Contorta Beds consists of illite (muscovite), chlorite, illite-smectite mixed layers, and kaolinite. In contrast, the Triletes Beds are significantly enriched in kaolinite, whereas in the Psilonotenton Formation the kaolinite content decreases again.

5.4. Bulk rock biogeochemical properties of the Tr–J transition beds

The $\delta^{13}C_{TOC}$ of the oldest beds of the Bonenburg section (Contorta Beds) fluctuates between –29.2 and –24.8‰ (Fig. 3). Above 13.5 m, at the transition of the Contorta Beds to the Triletes Beds, a sharp shift to 3.7‰ higher $\delta^{13}C_{TOC}$ values can be discerned. The up-section interval between 13.5 to 30 m records consistently stable $\delta^{13}C_{TOC}$ of around –23.3‰. A sharp shift to about 3.8‰ lower $\delta^{13}C_{TOC}$ marks the transition to more carbonate-rich strata of the Psilonotenton Formation. The succeeding up-section interval documents ^{13}C-depleted TOC, ranging between –30.0 and –25.4‰. Stratigraphic variations in $\delta^{13}C_{TOC}$ of the Kuhjoch section are signified by a pronounced negative shift to –31.2‰ at the height

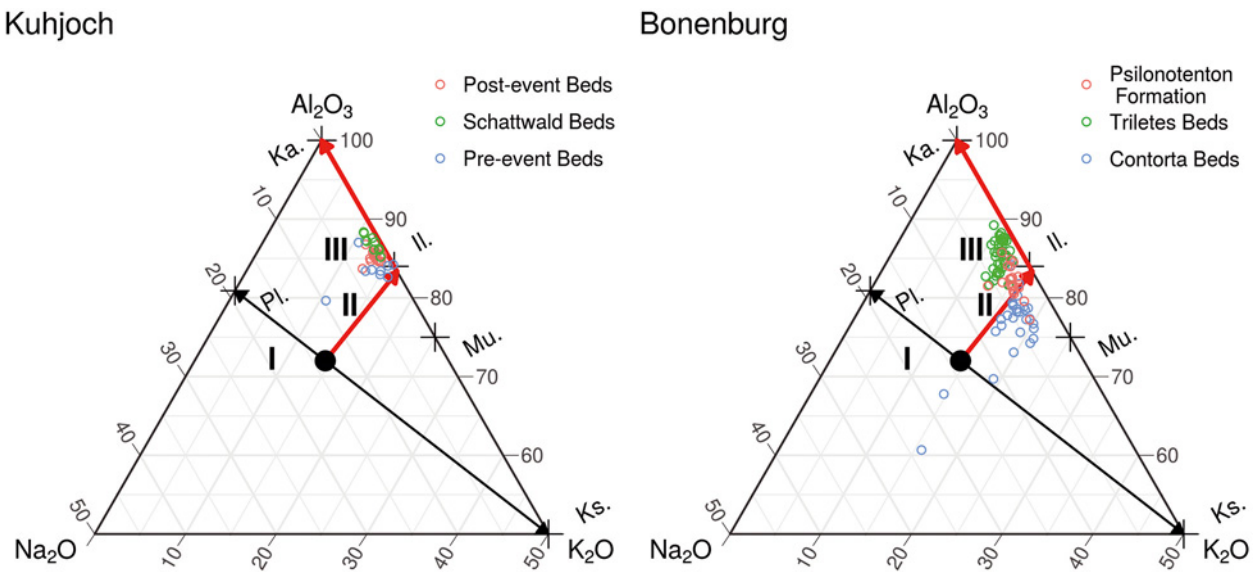

Fig. 5. Modified A–CN–K ternary diagram (cf. Nesbitt & Young 1984), plotting the molar proportions of Al_2O_3, Na_2O and K_2O. The characteristic upper continental crust composition is demarcated by a large black dot. Together with the minerals plagioclase (Pl.), K-feldspar (Ks.), muscovite (Mu.), illite (Il.) and kaolinite (Ka.), these values provide anchor points for evaluating the geochemical trends at Bonenburg and Kuhjoch. Trendlines are drawn for the initial source rock plagioclase to K-feldspar ratio (I), and for plagioclase weathering (II) which is considered to be the initial phase of weathering, based on the observation that K-feldspar is less susceptible to leaching. This is followed by intense weathering and subsequent loss of potassium, forming K-depleted clay minerals (III). Both the Schattwald Beds and Triletes Beds seem to have been sourced from the most intensely weathered substrates compared with the bracketing strata, which are marked by relatively higher concentrations of potassium and sodium.

of the T-Bed (data taken from Ruhl et al. 2009; Fig. 4). A return towards more positive values is followed by generally high and invariable values in the Schattwald Beds ($\delta^{13}C_{TOC}$: –25.1‰). After this, a second negative shift demarcates the transition to the Post-event Beds (Tiefengraben Member), followed by ^{13}C-depleted TOC values ($\delta^{13}C_{TOC}$: –28.5‰) until approximately 8 m above the T-Bed.

We present TOC and TN values on a carbonate-free basis (cfb) to mitigate variable dilution of the element concentrations by changing sediment carbonate content. In the Contorta Beds, TOC_{cfb} and TN_{cfb} average at 1.54 % and 0.07 %, respectively, and are highly variable, with pronounced peaks in TOC_{cfb} and TN_{cfb} in the upper part of the Contorta Beds (Fig. 3). By contrast, the Triletes Beds are depleted in TOC_{cfb} (0.26 %) and TN_{cfb} (0.04 %) and further stand out for their absence of significant variations. The lithological boundary of the Triletes Beds to the Psilonotenton Formation is again associated with pronounced peaks in TOC_{cfb} and TN_{cfb}, followed up-section by continued enrichment (TOC_{cfb}: 1.30 % and TN_{cfb}: 0.07 %) and variability. Stratigraphic variations in molar C/N (TOC/TN) and the marine palynomorph fraction follow to some extent TOC_{cfb} and TN_{cfb} modulations. Although published data on TN_{cfb} and C/N (data taken from Ruhl et al. 2010) are rather incomplete for large portions of the Kuhjoch section (Fig. 4), it is still noteworthy to mention that maxima in TOC_{cfb}, TN_{cfb} and C/N coincide within the T-Bed. More than half of the palynomorph assemblage consists of marine constituents in samples from the uppermost Pre-event Beds and the Post-event Beds of Kuhjoch, but this fraction (f_{marine} = marine palynomorphs/[marine + terrestrial palynomorphs]) is markedly depleted within the Schattwald Beds to values lower than 0.2. By contrast, f_{marine} values of 0.17±0.13 (mean and SD) are encountered in the Bonenburg material, with only minimal variation throughout the investigated sequence. In addition, palynomorphs make-up only 0.12±0.09 (mean and SD) of all counted organic particles ($f_{palynomorph}$ = palynomorphs/total organic particles), whereas wood particles account for 0.58±0.23 (mean and SD) of the organic debris in the Bonenburg material (f_{wood} = woods fragments/total organic particles).

6. Discussion

6.1. A correlative framework for the Central European Basin and the western Tethys shelf seas

Ammonite zonation: Hettangian ammonite biostratigraphy is well established for several regions in Central and Western Europe such as south-western England (e. g., Page & Bloos 1998, Bloos & Page 2000, Page 2002), northern Germany (e. g., Lange 1941), south-western Germany (e. g., Wetzel 1929, Blind 1963, Bloos 1999) and the NCA (e. g., Wähner 1886, Lange 1952, Blind 1963, Bloos 2004, von Hillebrandt & Krystyn 2009). Correlation of these regions showed that the Alpine successions are more complete than those of the other regions. Earliest Jurassic ammonite assemblages are characterized by *Psiloceras planorbis* (*Planorbis* Subchronozone; Trueman 1922) and in Great Britain can be subdivided into six biohorizons (Page & Bloos 1998, Page 2002). Less complete successions are known from northern Germany, where the "Psiloceras-Stufe" was subdivided into six zones with *Psiloceras psilonotum*, *Ps. plicatulum* and various species of *Neophyllites* characterizing the oldest zone (*Psiloceras psilonotum* Zone). In south-western Germany, Wetzel (1929, 1932), and Bloos (1999) identified three fossil assemblages beginning with (1) *Neophyllites imitans* and *N. antecedens*, (2) *Psiloceras psilonotum*, rare *Neophyllites becki* and *Ps. plicatulum*, and (3) *Caloceras franconicum* and *Curviceras subangulare*. In the NCA, Jurassic ammonite assemblages older than the *Planorbis* Chronozone were first recognized by von Hillebrandt & Krystyn (2009). In this respect, the Alpine sections more closely resemble successions in Nevada (Guex et al. 1998, 2004) and Chile (von Hillebrandt 2000) where assemblages are characterized by *Psiloceras spelae* and *Psiloceras tilmanni*.

Terrestrial palynomorph assemblages: Our palynological zonation mainly follows Lund (1977) with respect to the RL- and RP-assemblage zones. Minor differences are related to the Tr–J transition. Barth et al. (2018) suggested the new *Deltoidospora–Concavisporites* Zone (DC-Zone) to cross the Tr–J transition incorporating Lund's topmost upper Rhaetian and the lowermost part of the *Pinuspollenites–Trachysporites* Zone (PT-Zone). Although in Bonenburg a transitional phase, characterized by elements of both the RP- and the PiH-Zone is indicated in the uppermost part of the Triletes Beds, it does not show a continuous high abundance of *Deltoidospora* spp. and *Concavisporites* spp. typical for the new DC-Zone, nor a "transitional spore peak interval" as generally recorded in the CEB (Lund 1977, Barth et al. 2018), Sweden (Larsson 2009) and the Danish Basin (Lindström et al. 2017a). The increased dominance of pollen over spores can obscure changes in the spore assemblage. However, when examining changes only within the spore assemblage, it becomes apparent that the Bonenburg section depicts an increase in 'spores indet' along the transition from the RP- to the PiH-Zone. Considering the occurrence of aberrant *Deltoidospora* spp. and *Concavivsporites* spp. in the basal Hettangian, as documented in Barth et al. (2018), we cannot exclude that a number of aberrant *Deltoidospora* spp. and *Concavivsporites* spp. is included in 'spores indet' in our count that could have been included in these taxa as aberrant forms. Nevertheless, when comparing changes in the overall terrestrial assemblage, i. e. comparing pollen and spores (also incorporating spores indet) the Bonenburg section does not show the "spore peak" with the same amplitude as recorded by other authors (Lund 1977, Heunisch 2010, Lindström 2016, Barth et al. 2018).

The palynological zonation of the NCA (Kuerschner et al. 2007, Bonis et al. 2009, von Hillebrandt et al. 2013) correlates well with the zonation of the CEB (Barth et al. 2018), and this also holds for Bonenburg with minor differences. Comparison of Bonenburg with the zonation of Morbey (1975) for the Kendelbach section shows that the base of Morbey's TK Zone (i. e. the Me-subzone) is characterized by the appearance of *Perinosporites thuringiacus*, which in Bonenburg, after two singular occurrences in the RL-Zone, occurs continuously from the base of the RP-Zone. Compared to the NCA, *Trachysporites* spp. generally occurs in low abundances in Bonenburg. Low abundances of this genus were also reported from southern Sweden (Larsson 2009), and the respective zone is accordingly called *Pinuspollenites-Heliosporites* Zone, differing from the otherwise commonly used PT/TPi-Zone (Lund 1977, Kuerschner et al. 2007, Bonis et al. 2009, Heunisch et al. 2010, von Hillebrandt et al. 2013, Barth et al. 2018). Lund (1977) reported similarly scattered and rare occurrences of *Trachysporites* spp. in the Rhaetian and Hettangian of Eitzendorf close to Bonenburg. There seems to be a general tendency that in the CEB and in the British Rhaetian-Hettangian succession *Trachysporites* spp. is comparatively rare while *Deltoidospora* spp. is more

abundant (Lund 1977, Larsson 2009, Heunisch et al. 2010, Bonis et al. 2010, Barth et al. 2018), as opposed to the western Tethys shelf sections where *Trachysporites* spp. dominates over *Deltoidospora* spp. Another notable difference concerns the subdivision of the interval corresponding to the RP-Zone in the CEB. Kuerschner et al. (2007), Bonis et al. (2009) and von Hillebrandt et al. (2013) describe two zones for this interval: the *Rhaetipollis–Porcellispora* (RPo) Zone and *Trachysporites–Porcellispora* (TPo) Zone (see correlation schemes in Bonis et al. 2009, Lindström et al. 2017b, Barth et al. 2018). Like other CEB sections, Bonenburg does not show such changes in spore composition and apart from the described differences, the Bonenburg section correlates well with the western Tethys shelf sea sections.

Besides quantitative changes in whole terrestrial pollen assemblages, a few notable FOs and LOs of individual taxa characterize the Tr–J transition. These first and last occurrences can be used for correlations with the Alpine realm and beyond. Typical Triassic palynomorphs (e. g., *Lunatisporites rhaeticus*, *Triancoraesporites* spp.) are still present in the Kössen Formation and the Schattwald Beds. The records of these taxa show that they disappear at the top of the RPo-Zone. In St Audrie's Bay (UK), the LOs of these taxa are towards the top of the Cotham Member of the Lilstock Formation, although they do not disappear exactly synchronously at this level (Warrington et al. 1994, Hounslow et al. 2004, Warrington 2005, Bonis et al. 2010). In Bonenburg, the mentioned palynomorphs occur until the upper quarter of the Triletes Beds, which allows correlating the Schattwald Beds with the lower three quarters of the Triletes Beds.

These findings can be used for a provisional correlation of the CEB and the western Tethys shelf seas deposits and support previous correlations by Lindström et al. 2017b and Korte et al. (2019). This stratigraphic framework, primarily based on lithology, but supported by biostratigraphy, enables testing the facies-dependence of the TOC-carbon isotope composition in the Event Beds. Accordingly, in this framework, we suggest a synchronous deposition of the Contorta Beds and Pre-event Beds (of the NCA) and of the Triletes Beds and Schattwald Beds, respectively. However, the Tr–J transitional beds of Bonenburg, and many sites of the CEB, are incomplete around the transition from the Triletes Beds to the Psilonotenton Formation. Hence it remains unknown how the Psilonotenton Formation and the Post-event Beds of the NCA relate within this stratigraphic framework.

6.2. Organic matter sources and preservation

An evaluation of organic matter sources and preservation is required in order to determine the potential of stratigraphic $\delta^{13}C_{TOC}$ variations to faithfully represent temporal changes in the isotope composition of the Late Triassic to Early Jurassic atmosphere/ocean system. By establishing that the sections show distinct changes in lithology, floral and faunal composition and mineralogy, we highlight the necessity to evaluate the organic matter composition. A clay mineralogical shift to more K-depleted minerals in the Event Beds invokes a changing weathering regime that, in turn, could have been accompanied by an organic matter source shift, where, for instance, marine and terrestrial OC endmembers are usually characterized by different C isotope compositions (Arthur et al. 1985, Hayes et al. 1999, Strauss and Peters-Kottig 2003, Poole et al. 2004). Moreover, during greenhouse conditions the C isotope fractionation associated with metabolism of C3 land-plants is diminished, forming ^{13}C-enriched OC (Arthur et al. 1985, Strauss and Peters-Kottig 2003). Hence, an enhanced influx of terrestrial sourced organic compounds in a Tr–J greenhouse world could explain the ^{13}C-enriched Events Beds, and an assessment of the organic matter composition is therefore desirable.

The sediments' TOC and TN are frequently used parameters to assess the fidelity of $\delta^{13}C_{TOC}$, as they can allude to the primary OC sources (e. g., Ruhl et al. 2010). Especially the ratio of sedimentary C to N is often considered as a property to distinguish between the relative proportions of terrestrial and marine endmembers contributing to the total pool of organic matter, where marine organic matter is more-enriched in N-bearing compounds (C/N = 5–7) relative to terrestrial organics (C/N > 20) (De Lange 1992, Meyers 1994, Schubert & Calvert 2001). In a similar fashion, the palynological count data, in terms of the absolute or relative proportions of marine versus terrestrial elements, is considered to reflect the major contributing OC sources (e. g., Bonis et al. 2010). These parameters do, however, have inherent limitations, and an evaluation of their specific fidelity is required to assess their effectiveness in tracking source-induced stratigraphic $\delta^{13}C_{TOC}$ variations.

Crossplots of palynofacies, palynomorph, elemental and isotope data reveal distinct correlative trends, where $\delta^{13}C_{TOC}$ displays a pronounced negative correlation with TOC_{cfb}, reproducible for both localities

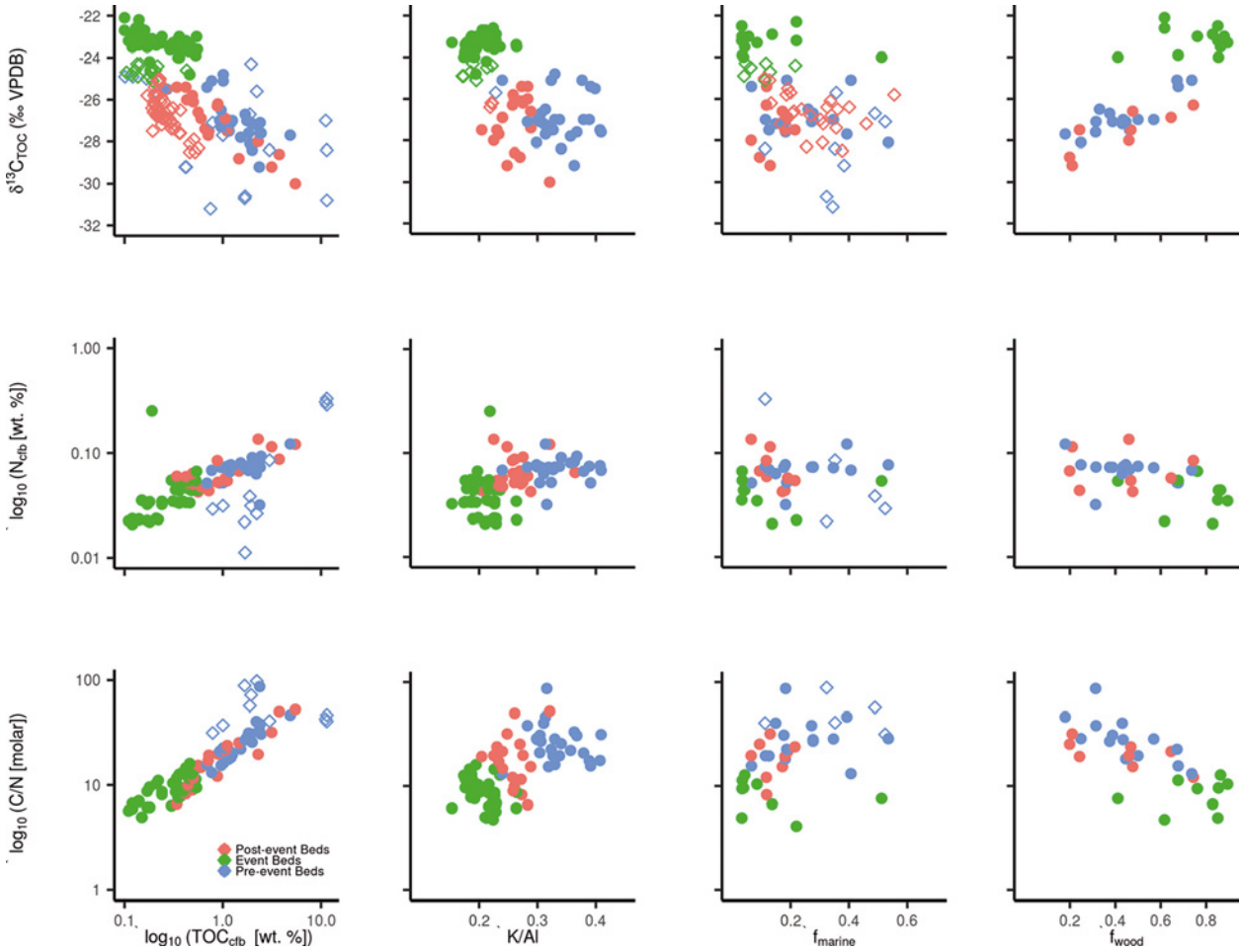

Fig. 6. Crossplots of $\delta^{13}C_{TOC}$, TN and C/N versus TOC, fraction of marine palynomorphs (marine palynomorphs/[marine + terrestrial palynomorphs]), fraction of wood fragments (woods fragments/total organic particles) and K/Al for Kuhjoch (diamonds) and Bonenburg (dots).

(Fig. 6 and Table 1). In addition, there is clear differentiation in the co-variance of $\delta^{13}C_{TOC}$ with TOC_{cfb} according to lithological units, where the Schattwald Beds and Triletes Beds plot in a distinctive area of the Cartesian coordinate system. These relationships suggest a control of the organic substrate on the C isotope composition. Significant positive linear trends can be observed between $\log_{10}(TOC_{cfb})$ and $\log_{10}(TN_{cfb})$ (Table 1) suggesting that these bio-essential elements have a common source, and an ad hoc interpretation would regard this feature to be representative for a lack of significant changes in the organic matter source. These simplistic views on C/N are complicated by the $\log_{10}$(C/N), which also positively correlates with $\log_{10}(TOC_{cfb})$ (Fig. 6 and Table 1). The linear relationships on a log-log plot for these parameters might approach a power law, and hence describe proportional changes across orders of magnitude. This suggests that stratigraphic trends towards elevated TOC and C/N are of a larger amplitude when compared with constituent TN variations which are relatively dampened. As such, the linear relationships on the log-log plots for TN–TOC and C/N–TOC can be explained by an increased input of organic matter that predispositions subsequent degradation of accumulated organic substrates towards more labile N-bearing organic matter compounds (Twichell et al. 2002, Arndt et al. 2013). Nevertheless, many factors determine the long-term diagenetic stabilization of sedimentary organic matter. For example, sedimentation rates, mineral surfaces, and sorption to minerals are potential factors that can control organic matter preservation (Hedges & Keil 1995).

Further complexities are evident in the co-variance of K/Al and $\log_{10}(TN_{cfb})$, which reveal a strong correlation and a clear separation of the sample space

Table 1 Results of linear model fitting.

Section	x	y	Intercept	Coefficient	r^2	p
Bonenburg	$\log_{10}(TOC_{cfb}$[wt.%])	$\delta^{13}C_{TOC}$	–26.35	–3.96	0.78	< 0.05
	$\log_{10}(TOC_{cfb}$[wt.%])	$\log_{10}(TN_{cfb}$[wt.%])	–1.21	0.38	0.60	< 0.05
	$\log_{10}(TOC_{cfb}$[wt.%])	$\log_{10}$(C/N [molar])	1.28	0.62	0.80	< 0.05
	K/Al [atomic]	$\delta^{13}C_{TOC}$	–19.79	–21.29	0.46	< 0.05
	K/Al [atomic]	$\log_{10}(TN_{cfb}$[wt.%])	–1.72	1.66	0.24	< 0.05
	K/Al [atomic]	$\log_{10}$(C/N [molar])	0.47	2.63	0.31	< 0.05
	f_{marine}	$\delta^{13}C_{TOC}$	–24.94	–4.72	0.09	0.07
	f_{marine}	$\log_{10}(TN_{cfb}$[wt.%])	–1.29	0.30	0.05	0.23
	f_{marine}	$\log_{10}$(C/N [molar])	16.41	28.91	0.06	0.17
	f_{wood}	$\delta^{13}C_{TOC}$	–29.78	7.24	0.67	< 0.05
	f_{wood}	$\log_{10}(TN_{cfb}$[wt. %])	–1.00	–0.44	0.28	< 0.05
	f_{wood}	$\log_{10}$(C/N [molar])	45.54	–43.88	0.41	< 0.05
Kuhjoch	$\log_{10}(TOC_{cfb}$[wt.%])	$\delta^{13}C_{TOC}$	–27.53	–2.18	0.35	< 0.05
	$\log_{10}(TOC_{cfb}$[wt.%])	$\log_{10}(TN_{cfb}$[wt.%])	–1.74	1.11	0.82	< 0.05
	$\log_{10}(TOC_{cfb}$[wt.%])	$\log_{10}$(C/N [molar])	1.81	–0.11	0.04	0.55
	K/Al [atomic]	$\delta^{13}C_{TOC}$	–21.25	–19.45	0.28	0.09
	f_{marine}	$\delta^{13}C_{TOC}$	–25.18	–5.55	0.27	< 0.05
	f_{marine}	$\log_{10}(TN_{cfb}$[wt.%])	–0.40	–2.30	0.63	0.11
	f_{marine}	$\log_{10}$(C/N [molar])	1.72	–0.11	0.01	0.87

according to the major lithological units (Fig. 6 and Table 1). Similar correlations have been related to the ability of ammonium to substitute for potassium in clay minerals, as the ionic radius of both cations is about the same (De Lange 1992). This non-exchangeable ammonium (or clay-bound NH_4^+) is most common in illite and rare in kaolinite. Comparably strong correlations between K/Al and nitrogen have been observed for modern marine sediments and have been explained by the illite content of these substrates. These patterns suggest that reduced illite content (relative to kaolinite) in the Triletes Beds could explain the depleted TN content. If correct, we can deduce that TN reflects the contribution of clay-bound ammonium, and the strong relation of TN with TOC has other underlying mechanisms than commonly inferred for non-fixed N sources. Weathering and sediment transport-related effects might be responsible for the diminished clay-bound N content of the Triletes Beds. With increased continental weathering (Zajzon et al. 2012), elevated siliciclastic input could have diluted the organic matter flux, thereby explaining the low TOC content of the Event Beds. Dilution of organic matter by siliciclastic material is a phenomenon observed in modern deltaic environments (Hedges & Keil 1995).

Relative contributions of marine versus terrestrial palynomorphs correlate poorly with $\delta^{13}C_{TOC}$ (Table 1), and variation of f_{marine} stays in a relatively narrow range (0.17±0.13 [mean and SD] of the total palynomorph pool, and $f_{palynomorphs}$ account for 0.12 ±0.09 [mean and SD] for Bonenburg, Fig. 3). Combined, these observations suggest that commonly made inferences, based on TOC, TN and the relative contribution of marine palynomorphs, are either inconclusive in identifying potential sedimentary OC source shifts, or invoke insignificant changes in the relative contribution of marine versus terrestrial OC, at least, within the framework of this study. This exercise therefore shows that TOC, TN, and the fraction of marine palynomorphs are less than perfect parameters to elucidate the source and diagenetic pathways of sedimentary organic carbon for this setting. Notable is the connection of clay mineralogy with TN and C/N, and the associated assertion that clay-bound NH_4^+ is an important source of N. This complicates inferences on the major source of organic matter, notably the relative contributions of marine versus terrestrial end-members. It, therefore, leaves open the question whether the precursor organic carbon pool was dominated by marine or terrestrial OC constituents.

The strong correlation of $\delta^{13}C_{TOC}$ and the fraction of wood fragments (Fig. 6 and Table 1), the abundance and relatively large range of f_{wood} (0.58±0.23 [mean and SD]), support a terrestrial-dominated OC pool for the Bonenburg section, or, at least, that a change in the composition of land-derived organic matter forced the stratigraphic variations in $\delta^{13}C_{TOC}$. Furthermore, a

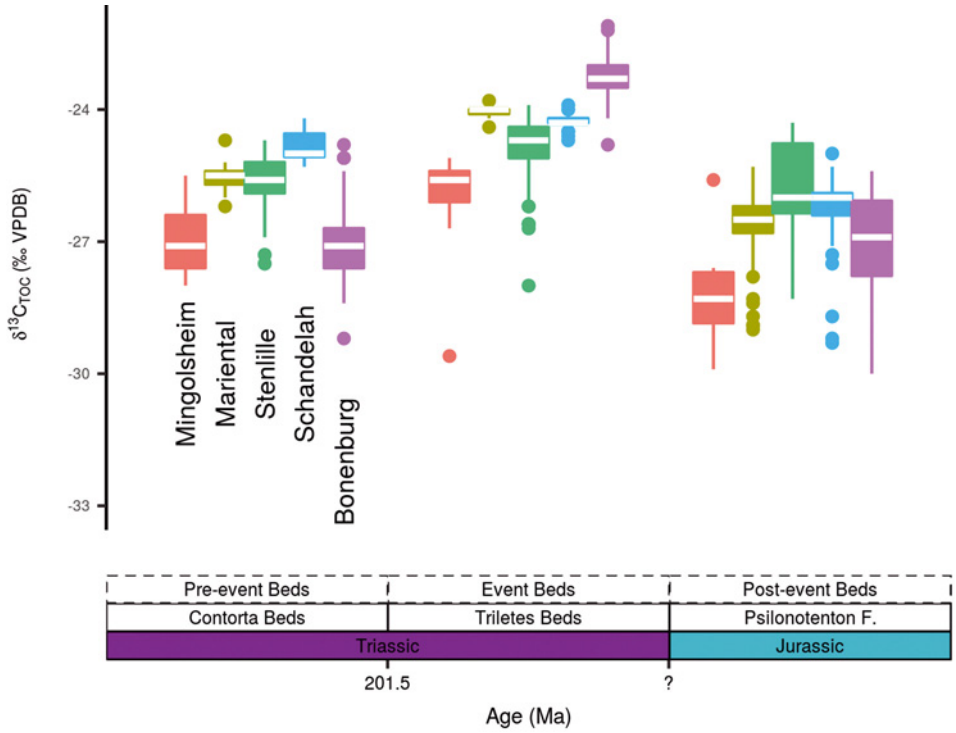

Fig. 7. Boxplots of $\delta^{13}C_{TOC}$ of the combined sites in the CEB binned for three stratigraphically distinct units (Section 5.1), compiling data from the Mingolsheim core (Quan et al. 2008), the Stenlille core (Lindström et al. 2012), the Mariental core (van de Schootbrugge et al. 2013), the Schandelah core (van de Schootbrugge et al. 2019) and the Bonenburg section (this study). Age of the lower boundary of the Triletes Beds is after Lindström et al. (2017 b) and Korte et al. (2019); the Tr–J is comprised by a hiatus in the CEB.

common pattern in the crossplots of $\delta^{13}C_{TOC}$ with K/Al is that the values of the Schattwald and the Triletes beds cluster in a distinct domain of the plot with relatively little scatter. This pattern suggests uniformity in the source of organic matter and clay minerals. By contrast the younger and older parts of the succession show more overlap and contain a more variable signal. This uniformity extends beyond Kuhjoch and Bonenburg to sections where similar trends in the clay mineral assemblages with an increase or predominance of kaolinite in the topmost Rhaetian beds occur in the NCA (Pálfy & Zajzon 2012, Zajzon et al. 2012) and in several other regions in Europe (Simms & Ruffell 1989, Ahlberg et al. 2003, Michalik et al. 2010, van de Schootbrugge et al. 2009, Bránski 2014, Nystuen et al. 2014). These similarities in first-order trends hint at a common temporal evolution of clay mineral formation and/or similar climate-driven weathering regime shift for these geographically distinct sites. In addition, compilations of $\delta^{13}C_{TOC}$ for the CEB (the Mingolsheim, Stenlille, Mariental and Schandelah cores; Fig. 7) and western Tethys shelf seas (the Restentalgraben, Tiefengraben, Kendlbachgraben and Hochalplgraben sections; Fig. 8) suggest that ^{13}C-enriched TOC with low variability is a shared characteristic for the Events Beds (Triletes and Schattwald beds). This is further corroborated by Kruskal-Wallis rank sum tests and Pairwise Wilcoxon rank sum tests, which show that the median $\delta^{13}C_{TOC}$ of the stratigraphic units are significantly different, except for the Contorta Beds and Psilonotenton Formation of Stenlille and Bonenburg which cannot be distinguished (Fig. 7). This observation fits within the chemostratigraphic correlation scheme of the Tr–J boundary interval which was recently reviewed by Korte et al. (2019).

6.3. Perspectives on TOC-carbon isotope based stratigraphic schemes

Transient negative excursions in $\delta^{13}C_{TOC}$ of the Tr–J boundary intervals have been linked to pronounced perturbations of the global carbon cycle, based on compound-specific C isotope analysis (Ruhl et al.

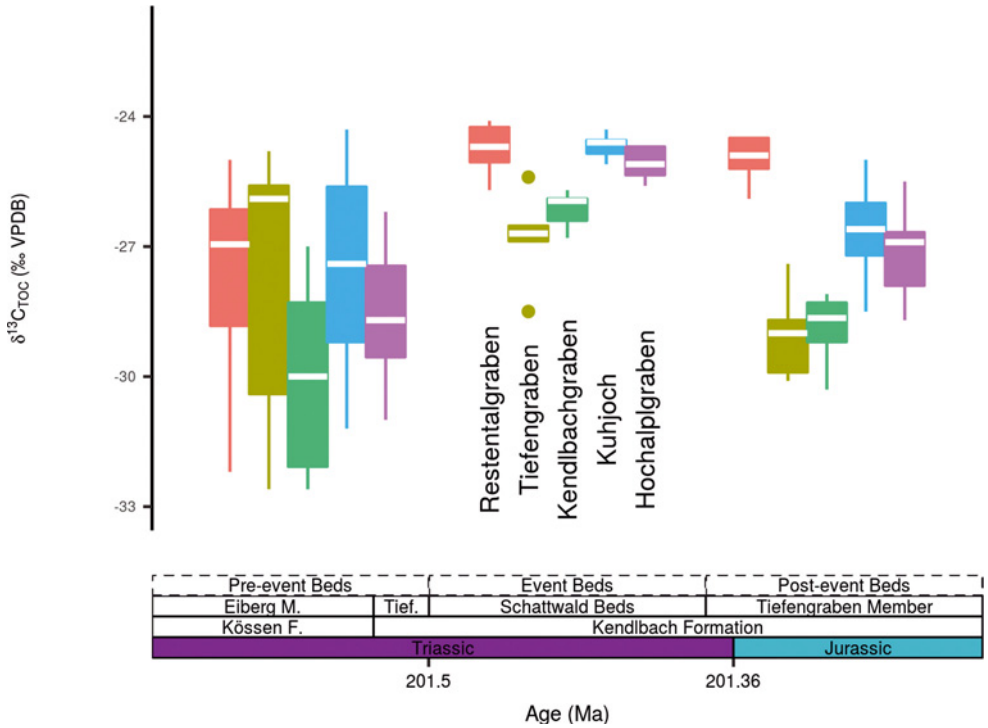

Fig. 8. Boxplots of $\delta^{13}C_{TOC}$ of the combined sites in the NCA binned for three stratigraphically distinct units (Section 5.2), compiling data from the Restentalgraben, Tiefengraben, Kendlbachgraben, Kuhjoch and Hochalplgraben sections (Kuerschner et al. 2007, Ruhl et al. 2009). The Kendlbachgraben and Tiefengraben lithological subdivision is based on clay mineralogy analysis by Zajzon et al. (2012) and a change to a more silty lithology (Kuerschner et al. 2007), respectively. Age of the lower Schattwald Beds is after Lindström et al. (2017 b) and Korte et al. (2019); the age of the Tr–J boundary is after Wotzlaw et al. (2014). (Tief. = Tiefengraben Member).

2011). By contrast, long-term $\delta^{13}C_{TOC}$ trends over the Tr–J transitional beds, and, in particular, the positive $\delta^{13}C_{TOC}$ signature of the Event Beds, have not undergone equivalent rigorous testing (see discussion in Bachan et al. 2012, Yager et al. 2017 for potential explanations for TOC ^{13}C-enrichment in the Event Beds).

The supra-regional TOC ^{13}C-enrichment in the Event Beds (Fig. 7 and Fig. 8) suggests a primary isotope signature, which traces the isotope composition of the exogenic carbon reservoir, which in turn is dictated by the fluxes in (volcanism and metamorphism-derived C) and out (burial of C) of the system. Furthermore, considering a 10^5 y duration of the Event Beds (Fig. 8 and Lindström et al. 2017b), the $\delta^{13}C_{TOC}$ should have originated from a well-mixed reservoir, as the residence time of carbon in the ocean-atmosphere system (10^5 y) is larger than the ocean mixing time (10^3 y) (Kump 1989, Dickens et al. 1995). It thus follows that the magnitude of the inflection to positive values should have been uniform across the whole ocean. However, this observation seems to be at odds with the variable magnitude of the observed C isotope shift (Fig. 7 and Fig. 8), and alternative explanations need to be explored.

Local $\delta^{13}C$ departures from the global C isotope signal could result from restricted seawater exchange of the basin with the open ocean (Holmden et al. 1998, Saltzman 2001, Bachan et al. 2012). Alternatively, spatial variations in the plankton community composition, and changes in the contributions of marine versus terrestrial components, can drive locally distinct sedimentary organic matter $\delta^{13}C$ signatures, which are produced by differences in C isotope fractionation associated with photosynthate production (Arthur et al. 1985, Farquhar et al. 1989, Meyers 1994, Kump & Arthur 1999). As marine palynomorph counts are potentially a poor reflection of the total sedimentary organic matter (where they represent only a small fraction of the organic particle pool, based on palynofacies analysis), a change in predominantly marine to terrestrial organic components can not entirely be discounted as the underlying cause for the ^{13}C-enriched values of the Event Beds. Nevertheless, a most

parsimonious scenario should also consider evidence of redox changes, and connected elevated levels of marine primary productivity, during the latest Rhaetian (Kasprak et al. 2015). These oceanic changes might relate to the collapse of terrestrial vegetation and elevated nutrient fluxes from the continents (Meyer et al. 2008, van de Schootbrugge et al. 2009, Algeo & Twitchett 2010, Kasprak et al. 2015). The synergistic effect of enhanced continental weathering and nutrient flux to the shelf environment favors a scenario of a change in the terrigenous OC flux over changes in the marine versus terrestrial end-member contribution. Combined with the ubiquity and highly variable occurrence of wood fragments in the Bonenburg section, these indices point towards a significant control of terrestrial-derived organic material on the $\delta^{13}C_{TOC}$ of the Tr–J transition beds. This interpretation is in accordance with previous studies of sections in the CEB and western Tethys shelf seas that employed kerogen characterization and compound specific C isotope analysis (van de Schootbrugge et al. 2009, Ruhl et al. 2010, Ruhl et al. 2011). In this case, $\delta^{13}C_{TOC}$ might reflect the isotope composition of atmospheric CO_2 (Strauss and Peters-Kottig 2003). However, small local deviations could arise from differences in the original organic matter transported from the continent to the seafloor (the organic debris of C_3 plants can range over several per mill in $\delta^{13}C$; O'Leary 1988, Cloern et al. 2002, Poole et al. 2004) and from differential trajectories of early diagenetic stabilization (Benner et al. 1987, Lehmann et al. 2002). Consistent with this reasoning, the co-variance of K/Al, and, in particular, the fraction wood fragments with $\delta^{13}C_{TOC}$, suggests that temporal $\delta^{13}C_{TOC}$ variations could equally be forced by source changes within the terrestrial OC flux.

The close correspondence of a clay mineralogy change, wood fragment abundance, and a shift to more ^{13}C-enriched TOC in the Event Beds therefore invokes a causal relationship. A change in the weathering regime might introduce more refractory terrestrial organic material ("pre-aged" or "fossil organic material" Meyers 1994) through increased physical erosion on land and an elevated riverine influx. A vegetation die-back and an enhanced hydrological cycle would be potential consequences of large-scale ecosystem destruction and greenhouse warming (van de Schootbrugge et al. 2009, Bonis et al. 2010, Ruhl et al. 2011), exposing and mobilizing previously untouched and mature organic matter sources. Additionally, a climatic shift to warmer and more humid conditions would have elevated chemical weathering rates, where episodic inundation could have catalyzed oxidative degradation of organic substrates (Hedges et al. 1999), leading to proportionally more refractory organic material transport to the depocenters. Such recalcitrant tissues (e. g., woody components) are known to harbor more positive C isotope signatures (O'Leary 1988, Jahren 2004, Cernusak et al. 2009, Schneebeli-Hermann et al. 2013). Hence, elevated contributions of recalcitrant organic material would be a viable pathway to drive $\delta^{13}C_{TOC}$ to higher values, a mechanism which should be explored in future studies on the Tr–J transitional beds. Factors such as the amount, source, and degradability of the original terrestrial organic compounds could be additional factors, which determine the ultimate TOC composition and could account for variations in the magnitude of the observed positive $\delta^{13}C_{TOC}$ shift. Intriguingly, the signal to more positive $\delta^{13}C_{TOC}$ is reproducible for different sites and even basins (e. g., Bachan et al. 2012, Blumenberg et al. 2016, Yager et al. 2017), potentially pointing toward a globally extensive event, which might still serve as a (regional) stratigraphic marker.

6.4. Statigraphic and environmental relevance of the Events Beds

The Event Beds have been a prime subject in recent studies (van de Schootbrugge et al. 2009, Pálfy & Zajzon 2012, Zajzon et al. 2012, Lindström et al. 2017b), which do not necessarily regard this unit to be the expression of sediment progradation forced by a sea level rise (Hallam & Wignall 1999). Instead the former mentioned studies infer an increased supply of siliciclastic sediments into the basin, possibly associated with more intense weathering under hot and humid greenhouse conditions. A fairly consistent positive $\delta^{13}C_{TOC}$ signature and the K-depleted clay mineral assemblage of the Event Beds further enforce this notion of a supra-regional event, where either climate-driven weathering intensification or a sudden terrigenous source change underlies the lithological transition. This sedimentary regime shift clearly differentiates the Event Beds from younger and older deposits.

The relevance of this sedimentary regime shift for palaeoenvironmental studies is twofold. First, increased sediment supply may result in dilution of micro- and macro-fossil assemblages and lead to the erroneous inference of a biological collapse. Facies-

dependent controls on fossil assemblages, and obtained quantitative estimates of stratigraphic ranges and diversity patterns, are a general concern in palaeontological studies (e. g., Patzkowsky & Holland 2012, Wang et al. 2014). Similarly, variable contributions of land-derived material, linked with elevated sediment rates, pose a problem for geochemical studies, as shown here for the stratigraphic potential of $\delta^{13}C_{TOC}$ and also for the interpretation of trace element enrichment patterns (e. g., Quan et al. 2008, Tanner et al. 2016). Second, elevated sediment fluxes are suggested to be a prime driver of the environmental perturbation at the Tr–J transition and other extinction events (e. g., the end-Permian mass extinction) by increasing water column turbidity and siltation which affected benthic filter-feeders on the shelf (Algeo & Twitchett 2010, Lindström et al. 2012), and by stimulating marine anoxia through elevated nutrient supply and increased levels of productivity (Meyer et al. 2008, Algeo & Twitchett 2010, Kasprak et al. 2015).

7. Conclusions

A robust stratigraphic framework is a prime prerequisite to understand the biotic and environmental changes at the Triassic–Jurassic boundary interval. Although carbon isotope records are a promising tool for global correlations by recording perturbations of the exogenic carbon reservoir as stratigraphic $\delta^{13}C$ fluctuations, multiple factors can bias this archive. Our study focused on stratigraphic TOC-based carbon isotope fluctuations in terms of their predominant contributors (i. e. organic matter sources versus the exogenic C pool) for key Tr–J sections. Lithology, macro-fossils and palynomorphs of the Bonenburg and Kuhjoch Tr–J transitional beds form a good basis to correlate these sites within their respective sedimentary basins, but also enable a tentative correlation between sections from the CEB and western Tethys shelf seas. Litho- and biostratigraphy of the Bonenburg site confirm the existence of a sedimentary hiatus in the upper Triletes Beds, which are unconformably overlain by the Psilonotenton Formation. This hiatus is a feature consistent among Tr–J sections of Northwestern Europe. Our mineralogical investigation reveals that the Event Beds (Triletes Beds and Schattwald Beds) are composed of K-depleted clay minerals (e. g., kaolinite), contrasting with the unit's bracketing lithology. This clay mineral shift is indicative of a terrigenous source change and/or a transition in the climate-controlled shift in the weathering regime. These outcomes corroborate previous interpretations suggesting that this lithological unit is an expression of the environmental changes during this time interval. However, these lithological and mineralogical indices also suggest that some stratigraphic $\delta^{13}C_{TOC}$ fluctuations could have been dictated by changes in the sourced organic matter (e. g., marine versus terrestrial OC contributions). A strong correlation between the dominant OC fraction consisting of wood and $\delta^{13}C_{TOC}$ invokes consideration of a causal effect. In such a scenario, the continentally derived organic matter becomes enriched in pre-aged or fossil organic matter, recycled from intensively weathered rock and soil sections. The degraded and selectively preserved products of terrestrial plants, such as wood fragments, are known to harbor a more positive $\delta^{13}C$ signature than more easily degradable products, thereby potentially explaining the ^{13}C-enriched TOC of the Event Beds. Even though it cannot be ruled out that this shift towards more positive $\delta^{13}C_{TOC}$ in the Event Beds is a perturbation of the exogenic C reservoir, the correlation of K-depleted clay mineralogy and ^{13}C-enriched TOC warrants revisiting current notions on the stratigraphic potential of TOC-based $\delta^{13}C$ records.

Acknowledgments. We acknowledge Joachim Thater of Lücking Ziegelwerke for permission to sample the Bonenburg section. We thank Martin Profft for assistance in faunal sampling and identifications, Michael Mertens for assistance in the field, and Manja Hethke for identification of conchostracans. We are indebted to Ralf Thomas Schmitt and Kathrin Krahn (Museum für Naturkunde Berlin) for performing the XRF element analysis on the samples. Marianne Falk (MfN, Berlin) is thanked for assistance with the carbon isotope analysis and Mufak S. Naoroz (University of Oslo) for assistance with palynological sample preparation. We are, furthermore, indebted to Thomas Borsch (Botanical Garden and Botanical Museum Berlin) for providing the microscope for palynofloral analysis and Julien Bachelier (Freie Universität Berlin) for proofreading as well as Martin Blumenberg (Bundesanstalt für Geowissenschaften und Rohstoffe) and an anonymous reviewer for constructive comments that significantly improved the manuscript. Funding was provided by the LWL-Museum für Naturkunde, Münster, Germany and by the MfN Innovationsfond (institute internal grant). This project is associated with the DFG Research Unit TERSANE (FOR 2332: Temperature-related stressors as a unifying principle in ancient extinctions).

References

Ahlberg, A., Olsson, I., Šimkevièius, P., 2003. Triassic-Jurassic weathering and clay mineral dispersal in basement areas and sedimentary basins of southern Sweden. Sedimentary Geology 161, 15–29.

Algeo, T. J., Twitchett, R. J., 2010. Anomalous Early Triassic sediment fluxes due to elevated weathering rates and their biological consequences. Geology 38, 1023–1026.

Arndt, S., Jørgensen, B. B., LaRowe, D. E., Middelburg, J. J., Pancost, R. D., Regnier, P., 2013. Quantifying the degradation of organic matter in marine sediments: A review and synthesis. Earth-Science Reviews 123, 53–86.

Arthur, M. A., Dean, W. E., Claypool, G. E., 1985. Anomalous ^{13}C enrichment in modern marine organic carbon. Nature 318, 216–218.

Auguie, B., 2017. GridExtra: Miscellaneous functions for "grid" graphics, https://cran.r-project.org/web/packages/gridExtra/index.html.

Bachan, A., Schootbrugge, B. van de, Fiebig, J., McRoberts, C. A., Ciarapica, G., Payne, J. L., 2012. Carbon cycle dynamics following the end-Triassic mass extinction: Constraints from paired $\delta^{13}C_{carb}$ and $\delta^{13}C_{org}$ records. Geochem. Geophys. Geosyst. 13, Q09008.

Bachmann, G. H., Voigt, T., Bayer, U., von Eynatten, H., Legler, B., Littke, R., 2008. Depositional history and sedimentary cycles in the Central European Basin System. In: Littke, R., Bayer, U., Gajewski, D., Nelskamp, S. (Eds.), Dynamics of Complex Sedimentary Basins. The Example of the Central European Basin System. Springer, 157–172.

Barth, G., Franz, M., Heunisch, C., Ernst, W., Zimmermann, J., Wolfgramm, M., 2018. Marine and terrestrial sedimentation across the T–J transition in the North German Basin. Palaeogeography, Palaeoclimatology, Palaeoecology 489, 74–94.

Benner, R., Fogel, M. L., Kent, S. E., Hodson, R. E., 1987. Depletion of ^{13}C in lignin and its implications for stable carbon isotope studies. Nature 329, 708–710.

Blind, W., 1963. Die Ammoniten des Lias alpha aus Schwaben, vom Fonsjoch und Breitenberg (Alpen) und ihre Entwicklung. Palaeontographica Abteilung A, 38–131.

Bloos, G., 1999. Neophyllites (Ammonoidea, Psiloceratidae) in the earliest Jurassic of South Germany. Neues Jahrbuch für Geologie und Paläontologie Abhandlungen 211, 7–29.

Bloos, G., 2004. Psiloceratids of the earliest Jurassic in the North-West European and Mediterranean Provinces: remarks and new observations. Stuttgarter Beiträge zur Naturkunde, Serie B (Geologie und Paläontologie) 347, 1–15.

Bloos, G., Page, K. N., 2000. The basal Jurassic ammonite succession in the north-west European province-review and new results. In: Hall, R., Smith, P. L. (Eds.), Advances in Jurassic Research 2000. Proceedings of the Fifth International Symposium on the Jurassic System. Georesearch Forum 6, 27–40.

Blumenberg, M., Heunisch, C., Lückge, A., Scheeder, G., Wiese, F., 2016. Photic zone euxinia in the central Rhaetian Sea prior the Triassic-Jurassic boundary. Palaeogeography, Palaeoclimatology, Palaeoecology 461, 55–64.

Bonis, N. R., Kürschner, W. M., Krystyn, L., 2009. A detailed palynological study of the Triassic-Jurassic transition in key sections of the Eiberg Basin (Northern Calcareous Alps, Austria). Review of Palaeobotany and Palynology 156, 376–400.

Bonis, N., Ruhl, M., Kürschner, W., 2010. Climate change driven black shale deposition during the end-Triassic in the western Tethys. Palaeogeography, Palaeoclimatology, Palaeoecology 290, 151–159.

Bránski, P., 2014. Climatic disaster at the Triassic-Jurassic boundary – a clay minerals and major elements record from the Polish Basin. Geological Quarterly 58, 291–310.

Broman, K. W., Broman, A. T., 2017, Broman: Karl broman's r code. R Package version 0.67-4. https://CRAN.R-project.org/package=broman.

Buggle, B., Glaser, B., Hambach, U., Gerasimenko, N., Marković, S., 2011. An evaluation of geochemical weathering indices in loess–paleosol studies. Quaternary International 240, 12–21.

Cernusak, L. A., Tcherkez, G., Keitel, C., Cornwell, W. K., Santiago, L. S., Knohl, A., Barbour, M. M., Williams, D. G., Reich, P. B., Ellsworth, D. S., Dawson, T. E., Griffiths, H. G., Farquhar, G. D., Wright, I. J., 2009. Viewpoint: Why are non-photosynthetic tissues generally ^{13}C enriched compared with leaves in C3 plants ? Review and synthesis of current hypotheses. Functional Plant Biology, 199–213.

Cloern, J., Canuel, E., Harris, D., 2002. Stable carbon and nitrogen isotope composition of aquatic and terrestrial plants of the San Francisco Bay estuarine system. Limnology and Oceanography 47, 713–729.

Dal Corso, J., Marzoli, A., Tateo, F., Jenkyns, H. C., Bertrand, H., Youbi, N., Mahmoudi, A., Font, E., Buratti, N., Cirilli, S., 2014. The dawn of CAMP volcanism and its bearing on the end-Triassic carbon cycle disruption. Journal of the Geological Society 171, 153–164.

De Lange, G. J., 1992. Distribution of exchangeable, fixed, organic and total nitrogen in interbedded turbiditic/pelagic sediments of the Madeira Abyssal-Plain, eastern North-Atlantic. Marine Geology 109, 95–114.

Dickens, G. R., Neil, J. R., Rea, D. K., Owen, R. M., 1995. Dissociation of oceanic methane hydrate as a cause of the carbon isotope excursion at the end of the Paleocene. Paleoceanography 10, 965–971.

Dunhill, A. M., Foster, W. J., Sciberras, J., Twitchett, R. J., 2018. Impact of the Late Triassic mass extinction on functional diversity and composition of marine ecosystems. Palaeontology 61, 133–148.

Farquhar, G. D., Ehleringer, J. R., Hubick, K. T., 1989. Carbon Isotope Discrimination and Photosynthesis. Annual Review: Plant Physiology Plant Molecular Biology 40, 503–537.

Fischer, J., Voigt, S., Franz, M., Schneider, J. W., Joachimski, M. M., Tichomirowa, M., Götze, J., Furrer, H., 2012. Palaeoenvironments of the late Triassic Rhaetian Sea:

Implications from oxygen and strontium isotopes of hybodont shark teeth. Palaeogeography, Palaeoclimatology, Palaeoecology 353–355, 60–72.

Fischer, V., Cappetta, H., Vincent, P., Garcia, G., Goolaerts, S., Martin, J. E., Roggero, D., Valentin, X., 2014. Ichthyosaurs from the French Rhaetian indicate a severe turnover across the Triassic–Jurassic boundary. Naturwissenschaften 101, 1027–1040.

Galli, T. M., Jadoul, F., Bernasconi, S. M., Weissert, H., 2005. Anomalies in global carbon cycling and extinction at the Triassic/Jurassic boundary: evidence from a marine C-isotope record. Palaeogeography, Palaeoclimatology, Palaeoecology 216, 203–214.

Golebiowski, R., 1990. The Alpine Kössen Formation, a key for European topmost Triassic correlations. Albertiana 8, 25–35.

Grimm, E., 2011. Tilia, TiliaGraph and TGView software, https://www.tiliait.com/.

Guex, J., Bartolini, A., Atudorei, V., Taylor, D., 2004. High-resolution ammonite and carbon isotope stratigraphy across the Triassic–Jurassic boundary at New York Canyon (Nevada). Earth and Planetary Science Letters 225, 29–41.

Guex, J., Bucher, H., Taylor, D., Rakus, M., 1998. Deux nouveaux genres et quatre nouvelles especes d'ammonites (Cephalopoda) du Lias inferieur. Bulletin de la Société vaudoise des Sciences naturelles 86, 73–85.

Hallam, A., 1981. The end-Triassic bivalve extinction event. Palaeogeography, Palaeoclimatology, Palaeoecology 35, 1–44.

Hallam, A., Wignall, P. B., 1999. Mass extinctions and sea-level changes. Earth Science Reviews 48, 217–250.

Hamilton, N., 2017. Ggtern: An extension to 'ggplot2', for the creation of ternary diagrams, https://rdrr.io/cran/ggtern/.

Hayes, J. M., Strauss, H., Kaufman, A. J., 1999. The abundance of ^{13}C in marine organic matter and isotopic fractionation in the global biogeochemical cycle of carbon during the past 800 Ma. Chemical Geology 161, 103–125.

Hedges, J. I., Keil, R. G., 1995. Sedimentary organic matter preservation: an assessment and speculative synthesis. Marine Chemistry 49, 81–115.

Hedges, J. I., Hu, F. S., Devol, A. H., Hartnett, H. E., Tsamakis, E., Keil, R. G., 1999. Sedimentary organic matter preservation: A test for selective degradation under oxic conditions. American Journal of Science 299, 529–555.

Hesselbo, S. P., Robinson, S. A., Surlyk, F., 2004. Sea-level change and facies development across potential Triassic–Jurassic boundary horizons, SW Britain. Journal of the Geological Society 161, 365–379.

Hesselbo, S. P., Robinson, S. A., Surlyk, F., Piasecki, S., 2002. Terrestrial and marine mass extinction at the Triassic/Jurassic boundary synchronized with initiation of massive volcanism. Geology 30, 251–254.

Heunisch, C., Luppold, F. W., Reinhardt, L., Röhling, H.-G., 2010. Palynofazies, Bio- und Lithostratigrafie im Grenzbereich Trias/Jura in der Bohrung Mariental 1 (Lappwaldmulde, Ostniedersachsen). Zeitschrift der Deutschen Gesellschaft für Geowissenschaften 161, 51–98.

Holmden, C., Creaser, R. A., Muehlenbachs, K., Leslie, S. A., Bergström, S. M., 1998. Isotopic evidence for geochemical decoupling between ancient epeiric seas and bordering oceans: implications for secular curves. Geology 26, 567–570.

Hounslow, M. W., Posen, P. E., Warrington, G., 2004. Magnetostratigraphy and biostratigraphy of the Upper Triassic and lowermost Jurassic succession, St. Audrie's Bay, UK. Palaeogeography, Palaeoclimatology, Palaeoecology 213, 331–358.

Hönisch, B., Ridgwell, A., Schmidt, D. N., Thomas, E., Gibbs, S. J., Sluijs, A., Zeebe, R., Kump, L., Martindale, R. C., Greene, S. E., Kiessling, W., Ries, J., Zachos, J. C., Royer, D. L., Barker, S., Marchitto, T. M., Moyer, R., Pelejero, C., Ziveri, P., Foster, G. L., Williams, B., 2012. The geological record of ocean acidification. Science 335, 1058–1063.

Ivimey-Cook, H., Hodges, P., Swift, A., Radley, J., 1999. Bivalves. In: Swift, A., Martill, D. M. (Eds.), Fossils of the Rhaetian Penarth Group. The Palaeontological Association, London, 83–127.

Jahren, H. A., 2004. The carbon stable isotope composition of pollen. Review of Palaeobotany and Palynology 132, 291–313.

Jüngst, H., 1928. Rät, Psilonoten- und Schlotheimienschichten im nördlichen Harzvorlande. PhD thesis, Friedrich-Wilhelms-Universität zu Berlin, 194 p.

Karle, U., 1984. Palynostratigraphische Untersuchung eines Rhät/Lias-Profils am Fonsjoch, Achensee (Nördliche Kalkalpen, Österreich). Mitteilungen der Österreichischen Geologischen Gesellschaft 77, 331–353.

Kasprak, A. H., Sepúlveda, J., Price-Waldman, R., Williford, K. H., Schoepfer, S. D., Haggart, J. W., Ward, P. D., Summons, R. E., Whiteside, J. H., 2015. Episodic photic zone euxinia in the northeastern Panthalassic Ocean during the end-Triassic extinction. Geology 43, 307–310.

Kiessling, W., Aberhan, M., Brenneis, B., Wagner, P. J., 2007. Extinction trajectories of benthic organisms across the Triassic-Jurassic boundary. Palaeogeography, Palaeoclimatology, Palaeoecology 244, 201–222.

Klaus, W. von, 1960. Sporen der Karnischen Stufe der ostalpinen Trias. Geologisches Jahrbuch der Geologischen Bundesanstalt 5, 107–184.

Klompmaker, A. A., Herngreen, W. G. F., Oosterink, H. W., 2010. Biostratigraphic correlation, paleoenvironment stress, and suberosion pipe collapse: Dutch Rhaetian shales uncover their secrets. Facies 56, 597–613.

Konietzko-Meier, D., Werner, J. D., Wintrich, T., Sander, P. M., 2018. A large temnospondyl humerus from the Rhaetian (Late Triassic) of Bonenburg (Westphalia, Germany) and its implications for temnospondyl extinction. Journal of Iberian Geology online early, 14 p.

Konhauser, K. O., Schiffman, P., Fisher, Q. J., 2002. Microbial mediation of authigenic clays during hydrothermal alteration of basaltic tephra, Kilauea Volcano. Geochemistry, Geophysics, Geosystems 3, 1–13.

Koohafkan, M. C., 2015. Kfigr: Integrated code chunk anchoring and referencing for RMarkdown documents, https://rdrr.io/cran/kfigr/.

Korneisel, D., Gallois, R. W., Duffin, C. J., Benton, M. J., 2015. Latest Triassic marine sharks and bony fishes from a bone bed preserved in a burrow system, from Devon, UK. Proceedings of the Geologists' Association 126, 130–142.

Korte, C., Ruhl, M., Palfy, J., Ullmann, C. V., Hesselbo, S. P., 2019. Chemostratigraphy across the Triassic-Jurassic boundary. In: Sial, A. N., Gaucher, C., Ramkumar, M., Ferreira, V. P. (Eds.), Chemostratigraphy across major chronological boundaries. Geophysical Monograph 240, 185–210.

Kozur, H. W., Weems, R. E., 2010. The biostratigraphic importance of conchostracans in the continental Triassic of the northern hemisphere. Geological Society, London, Special Publications 334, 315–417.

Krystyn, L., Bohm, F., Kurschner, W., Delecat, S., 2005. Field trip in Austria The Triassic – Jurassic boundary in the Northern Calcareous Alps. In: Pálfy, J., Ozsvárt, P. (Eds.), Program, Abstracts and Field Guide. 5th Field Workshop of IGCP 458 Project. Tata and Hallein, A1–A14.

Kuerschner, W. M., Bonis, N. R., Krystyn, L., 2007. Carbon-isotope stratigraphy and palynostratigraphy of the Triassic-Jurassic transition in the Tiefengraben section – Northern Calcareous Alps (Austria). Palaeogeography, Palaeoclimatology, Palaeoecology 244, 257–280.

Kump, L. R., 1989. Alternative modeling approaches to the geochemical cycles of carbon, sulfur, and strontium isotopes. American Journal of Science 289, 390–410.

Kump, L. R., Arthur, M. A., 1999. Interpreting carbon-isotope excursions: carbonates and organic matter. Chemical Geology 161, 181–198.

Lange, W., 1941. Die Ammonitenfauna der Psiloceras-Stufe Norddeutschlands. Palaeontographica Abteilung A, 1–192.

Lange, W., 1952. Der untere Lias am Fonsjoch (östliches Karwendelgebirge) und seine Ammonitenfauna. Palaeontographica Abteilung A, 49–162.

Larsson, L. M., 2009. Palynostratigraphy of the Triassic-Jurassic transition in southern Sweden. GFF 131, 147–163.

Lehmann, M., Bernasconi, S., Barbieri, A., McKenzie, J., 2002. Preservation of organic matter and alteration of its carbon and nitrogen isotope composition during simulated and in situ early sedimentary diagenesis. Geochimica et Cosmochimica Acta 66, 3573–3584.

Lindström, S., Erlström, M., 2007. The late Rhaetian transgression in southern Sweden: Regional (and global) recognition and relation to the Triassic–Jurassic boundary. Palaeogeography, Palaeoclimatology, Palaeoecology 241, 339–372.

Lindström, S., Erlström, M., Piasecki, S., Nielsen, L. H., Mathiesen, A., 2017a. Palynology and terrestrial ecosystem change of the Middle Triassic to lowermost Jurassic succession of the eastern Danish Basin. Review of Palaeobotany and Palynology 244, 65–95.

Lindström, S., Pedersen, G. K., Schootbrugge, B. van de, Hansen, K. H., Kuhlmann, N., Thein, J., Johansson, L., Petersen, H. I., Alwmark, C., Dybkjær, K., Weibel, R., Erlström, M., Nielsen, L. H., Oschmann, W., Tegner, C., 2015. Intense and widespread seismicity during the end-Triassic mass extinction due to emplacement of a large igneous province. Geology 43, 387–390.

Lindström, S., Schootbrugge, B. van de, Dybkjær, K., Pedersen, G. K., Fiebig, J., Nielsen, L. H., Richoz, S., 2012. No causal link between terrestrial ecosystem change and methane release during the end-Triassic mass extinction. Geology 40, 531–534.

Lindström, S., van de Schootbrugge, B., Hansen, K. H., Pedersen, G. K., Alsen, P., Thibault, N., Dybkjær, K., Bjerrum, C. J., Nielsen, L. H., 2017b. A new correlation of Triassic–Jurassic boundary successions in NW Europe, Nevada and Peru, and the Central Atlantic Magmatic Province: A time-line for the end-Triassic mass extinction. Palaeogeography, Palaeoclimatology, Palaeoecology 478, 80–102.

Lomax, D., De la Salle, P., Massare, J., Gallois, R., 2018. A giant Late Triassic ichthyosaur from the UK and a reinterpretation of the Aust Cliff 'dinosaurian' bones, PLoS ONE 113, e0194742.

Lund, J. J., 1977. Rhaetic to Lower Liassic palynology of the onshore south-eastern North Sea Basin. Danmarks og Geologiske Undersøgelse 109, 1–129.

Mander, L., Twitchett, R., Benton, M., 2008. Palaeoecology of the Late Triassic extinction event in the SW UK. Journal of the Geological Society London 165, 319–332.

Marzoli, A., Callegaro, S., Corso, J. D., Davies, J. H. F. L., Chiaradia, M., Youbi, N., Reisberg, L., Merle, R., Jourdan, F., 2018. The Central Atlantic Magmatic Province (CAMP): A Review. In: Tanner, L. (Ed.), The Late Triassic World, Topics in Geobiology 46, Springer, 91–125.

McElwain, J. C., Beerling, D. J., Woodward, F. I., 1999. Fossil plants and global warming at the Triassic-Jurassic boundary. Science 285, 1386–1390.

Mears, E. M., Rossi, V., MacDonald, E., Coleman, G., Davies, T. G., Arias-Riesgo, C., Hildebrand, C., Thiel, H., Duffin, C. J., Whiteside, D. I., Benton, M. J., 2016. The Rhaetian (Late Triassic) vertebrates of Hampstead Farm Quarry, Gloucestershire, UK. Proceedings of the Geologist' Association 127, 478–505.

Meyer, K., Kump, L., Ridgwell, A., 2008. Biogeochemical controls on photic-zone euxinia during the end-Permian mass extinction. Geology 36, 747–750.

Meyers, P. A., 1994. Preservation of elemental and isotopic source identification of sedimentary organic matter. Chemical Geology 114, 289–302.

Michalik, J., Biron, A., Lintnerova, O., Götz, A., Ruckwied, K., 2010. Climate change at the Triassic-Jurassic boundary in the northwestern Tethyan realm, inferred from sections in the Tatra Mountains (Slovakia). Acta Geologica Polonica 60, 535–548.

Michalopoulos, P., Aller, R. C., 2004. Early diagenesis of biogenic silica in the Amazon delta: Alteration, authi-

genic clay formation, and storage. Geochimica et Cosmochimica Acta 68, 1061–1085.

Morbey, S. J., 1975. The palynostratigraphy of the Rhaetian stage, Upper Triassic in the Kendelbachgraben, Austria. Palaeontographica Abteilung B 152, 1–75.

Nielsen, L., 2003. Late Triassic – Jurassic development of the Danish Basin and the Fennoscandian Border Zone, southern Scandinavia. Geological Survey of Denmark And Greenland Bulletin 526, 459–526.

Nesbitt, H. W., Young, G. M., 1984. Prediction of some weathering trends of plutonic and volcanic-rocks based on thermodynamic and kinetic considerations. Geochimica et Cosmochimica Acta 48, 1523–1534.

Nilsson, T., 1958. Über das Vorkommen eines mesozoischen Sapropelgesteins in Schonen. Acta Universitatis Lundensis 54, 1–109.

Nystuen, J. P., Kjemperud, A. V., Müller, R., Adestål, V., Schomacker, E. R., 2014. Late Triassic to Early Jurassic climate change, northern North Seas region: impact on alluvial architecture, palaeosols and clay mineralogy. IAS Special Publications 46, 59–100.

O'Leary, M. H., 1988. Carbon isotopes in photosynthesis. Science 38 (5), 328–336.

Page, K. N., 2002. A review of the ammonite faunas and standard zonation of the Hettangian and Lower Sinemurian succession (Lower Jurassic) of the east Devon coast (south west England). Geoscience in south west England 10, 293–303.

Page, K. N., Bloos, G., 1998. The base of the Jurassic System in west Somerset, south-west England-New observations on the succession of ammonite faunas of the lowest Hettangian Stage. Proceedings of the Ussher Sociey 9, 231–235.

Patzkowsky, M. E., Holland, S. M., 2012. Stratigraphic Paleobiology: Understanding the distribution of fossil taxa in time and space, University of Chicago Press, 259 p.

Pálfy, J., Demény, A., Haas, J., Hetényi, M., Orchard, M. J., Vető, I., 2001. Carbon isotope anomaly and other geochemical changes at the Triassic-Jurassic boundary from a marine section in Hungary. Geology 29, 1047–150.

Pálfy, J., Zajzon, N., 2012. Environmental changes across the Triassic-Jurassic boundary and coeval volcanism inferred from elemental geochemistry and mineralogy in the Kendlbachgraben section (Northern Calcareous Alps, Austria). Earth and Planetary Science Letters 335–336, 121–134.

Pedersen, K. R., Lund, J. J., 1980. Palynology of the Plant-Bearing Rhaetian to Hettangian Kap Stewart Formation, Scoresby Sund, East Greenland. Review of Palaeobotany and Palynology 31, 1–69.

Popp, B. N., Takigiku, R., Hayes, J. M., Louda, J. W., Baker, E. W., 1989. The Post-Paleozoic chronology and mechanisms of ^{13}C depletion in primary marine organic matter. American Journal of Science 289, 436–454.

Quan, T. M., Schootbrugge, B. van de, Field, M. P., Rosenthal, Y., Falkowski, P. G., 2008. Nitrogen isotope and trace metal analyses from the Mingolsheim core (Germany): Evidence for redox variations across the Triassic-Jurassic boundary. Global Biogeochemical Cycles 22, 1–14.

R Core Team, 2018. R: A language and environment for statistical computing. R Foundation for Statistical Computing, Vienna, Austria, https://cran.r-project.org/.

Raup, D. M., Sepkoski, Jr. J. J., 1982. Mass extinctions in the marine fossil record. Science 215, 10–12.

Ruhl, M., Bonis, N. R., Reichart, G.-J., Sinninghe Damsté, J. S., Kürschner, W. M., 2011. Atmospheric carbon injection linked to end-Triassic mass extinction. Science 333, 430–434.

Ruhl, M., Kürschner, W. M., Krystyn, L., 2009. Triassic-Jurassic organic carbon isotope stratigraphy of key sections in the western Tethys realm (Austria). Earth and Planetary Science Letters 281, 169–187.

Ruhl, M., Veld, H., Kürschner, W. M., 2010. Sedimentary organic matter characterization of the Triassic-Jurassic boundary GSSP at Kuhjoch (Austria). Earth and Planetary Science Letters 292, 17–26.

Saltzman, M. R., 2001. Late Paleozoic ice age; Oceanic gateway or pCO_2?. Geology 31, 151–154.

Sander, P. M., Wintrich, T., Schwermann, A. H., Kindlimann, R., 2016. Die paläontologische Grabung in der Rhät-Lias-Tongrube der Fa. Lücking bei Warburg-Bonenburg (Kr. Höxter) im Frühjahr 2015. Geologie und Paläontologie in Westfalen 88, 11–37.

Schneebeli-Hermann, E., Kürschner, W. M., Hochuli, P. A., Ware, D., Weissert, H., Bernasconi, S. M., Roohi, G., Ur-Rehman, K., Goudemand, N., Bucher, H., 2013. Evidence for atmospheric carbon injection during the end-Permian extinction. Geology 41, 579–582.

Schobben, M., 2011. Marine and terrestrial proxy records of environmental changes across the Triassic/Jurassic transition: A combined geochemical and palynological approach. MSc-thesis, 49 p. (https://dspace.library.uu.nl/bitstream/handle/1874/207821/Marine%20and%20terrestrial%20proxy%20records%20of%20environmental%20changes%20across%20the%20TriassicJurassic%20transition.pdf?sequence=1&isAllowed=y).

Schubert, C. J., Calvert, S. E., 2001. Nitrogen and carbon isotopic composition of marine and terrestrial organic matter in Arctic Ocean sediments. Deep-Sea Research 48, 789–810.

Schulz, E., 1962. Sporenpaläontologische Untersuchungen zur Rhät-Lias-Grenze in Thüringen und der Altmark. Geologie 3, 308–319.

Schulz, E, 1967. Sporenpaläontologische Untersuchungen rätoliassischer Schichten im Zentralteil des Germanischen Beckens. Paläontologische Abhandlungen Abteilung B, 541–633.

Schuurman, W. M. L., 1976. Aspects of Late Triassic palynology. 1. On the morphology, taxonomy and stratigraphical/geographical distribution of the form genus Ovalipollis. Review of Palaeobotany and Palynology 21, 241–266.

Simms, M., Ruffell, A., 1989. Synchroneity of climatic change and extinctions in the Late Triassic. Geology 17, 265–268.

Storrs, G. W., 1994. Fossil vertebrate faunas of the British Rhaetian. Zoological Journal of the Linnean Society 112, 217–259.

Strauss, H., Peters-Kottig, W., 2003. The Paleozoic to Mesozoic carbon cycle revisited: The carbon isotopic composition of terrestrial organic matter. Geochemistry, Geophysics, Geosystems 4, 1083, doi: 10.1029/2003GC000555.

Tanner, L. H., Kyte, F. T., Richoz, S., Krystyn, L., 2016. Distribution of iridium and associated geochemistry across the Triassic-Jurassic boundary in sections at Kuhjoch and Kendlbach, Northern Calcareous Alps, Austria. Palaeogeography, Palaeoclimatology, Palaeoecology 449, 13–26.

Tanner, L. H., Lucas, S. G., Chapman, M. G., 2004. Assessing the record and causes of Late Triassic extinctions. Earth-Science Reviews 65, 103–139.

Trueman, A. E., 1922. The Liassic rocks of Glamorgan. Proceedings of the Geologists' Association 33, 245–284.

Twichell, S. C., Meyers, P. A., Diester-Haass, L., 2002. Significance of high C/N ratios in organic-carbon-rich Neogene sediments under the Benguela Current upwelling system. Organic Geochemistry 33, 715–722.

van de Schootbrugge, B., Bachan, A., Suan, G., Richoz, S., Payne, J. L., 2013. Microbes, mud and methane: Cause and consequence of recurrent early Jurassic anoxia following the end-Triassic mass extinction. Palaeontology 56, 685–709.

van de Schootbrugge, B., Payne, J. L., Tomasovych, A., Pross, J., Fiebig, J., Benbrahim, M., Föllmi, K. B., Quan, T. M., 2008. Carbon cycle perturbation and stabilization in the wake of the Triassic-Jurassic boundary mass-extinction event. Geochemistry, Geophysics, Geosystems 9, 1525–2027.

van de Schootbrugge, B., Quan, T. M., Lindström, S., Püttmann, W., Heunisch, C., Pross, J., Fiebig, J., Petschick, R., Röhling, H.-G., Richoz, S., Rosenthal, Y., Falkowski, P. G., 2009. Floral changes across the Triassic/Jurassic boundary linked to flood basalt volcanism. Nature Geoscience 2, 589–594.

van de Schootbrugge, B., Richoz, S., Pross, J., Luppold, F., Hunze, S., Wonik, T., Blau, J., Meister, C., Weijst, C. van der, Suan, G., Fraguas, A., Fiebig, J., Herrle, J., Guex, J., Little, C., Wignall, P., Püttmann, W., Oschmann, W., 2019. The Schandelah Scientific Drilling Project: A 25-million year record of Early Jurassic palaeo-environmental change from northern Germany. Newsletters on Stratigraphy 52.

van de Schootbrugge, B., Tremolada, F., Rosenthal, Y., Bailey, T. R., Feist-Burkhardt, S., Brinkhuis, H., Pross, J., Kent, D. V., Falkowski, P. G., 2007. End-Triassic calcification crisis and blooms of organic-walled 'disaster species'. Palaeogeography, Palaeoclimatology, Palaeoecology 244, 126–141.

von Hillebrandt, A., 2000. Die Ammoniten-Fauna des südamerikanischen Hettangium (basaler Jura) Teil III. Palaeontographica Abteilung A, 65–116.

von Hillebrandt, A., Krystyn, L., 2009. On the oldest Jurassic ammonites of Europe (Northern Calcareous Alps, Austria) and their global significance. Neues Jahrbuch für Geologie und Paläontologie Abhandlungen 253, 163–195.

von Hillebrandt, A., Krystyn, L., Kürschner, W., Bonis, N., Ruhl, M., Richoz, S., Schobben, M. A. N., Urlichs, M., Bown, P., Kment, K., McRoberts, C., Simms, M., Tomãsových, A., 2013. The Global Stratotype Sections and Point (GSSP) for the base of the Jurassic System at Kuhjoch (Karwendel Mountains, Northern Calcareous Alps, Tyrol, Austria). Episodes 36, 162–198.

Ward, P. D., Haggart, J. W., Carter, E. S., Wilbur, D., Tipper, H. W., Evans, T., 2001. Sudden productivity collapse associated with the Triassic-Jurassic boundary mass extinction. Science 292, 1148–1151.

Wang, Y., Sadler, P. M., Shen, S. Z., Erwin, D. H., Zhang, Y. C., Wang, X. D., Wang, W., Crowley, J. L., Henderson, C. M., 2014. Quantifying the process and abruptness of the end-Permian mass extinction. Paleobiology 40, 113–129.

Warrington, G., 2005. The Charmouth 16A Borehole, Dorset, U. K.: Palynology of the Penarth Group and the Basal Lias Group (Upper Triassic – Lower Jurassic). Geoscience in south-west England 11, 109–116.

Warrington, G., Cope, J. C. W., Ivimey-Cook, H. C., 1994. St. Audrie's Bay, Somerset, England: a candidate Global Stratotype Section and Point for the Base of the Jurassic. Geological Magazine 131, 191–200.

Wähner, F., 1886. Beiträge zur Kenntniss der tieferen Zonen des unteren Lias in den nordöstlichen Alpen. Beiträge zur Paläontologie Österreich-Ungarns und des Orients, 135–226.

Wetzel, R., 1929. Grenzprobleme zwischen Geologie und Paläontologie. Verhandlungen der physikalisch-medizinischen Gesellschaft zu Würzburg, Neue Folge 54, 178–187.

Wetzel, R., 1932. Leitfossil gegen Leithorizont und die mittelwürttembergische Psilonotenbank. Neues Jahrbuch für Mineralogie, Geologie und Paläontologie 67, 455–467.

Whiteside, J. H., Olsen, P. E., Eglinton, T., Brookfield, M. E., Sambrotto, R. N., 2010. Compound-specific carbon isotopes from Earth's largest flood basalt eruptions directly linked to the end-Triassic mass extinction. Proceedings of the National Academy of Sciences 107, 6721–6725.

Whiteside, J. H., Olsen, P. E., Kent, D. V., Fowell, S. J., Et-Touhami, M., 2007. Synchrony between the Central Atlantic magmatic province and the Triassic-Jurassic mass-extinction event? Palaeogeography, Palaeoclimatology, Palaeoecology 244, 345–367.

Wickham, H., 2009. ggplot2: Elegant graphics for data analysis, Springer-Verlag New York, https://cran.r-project.org/web/packages/ggplot2/index.html.

Wintrich, T., Hayashi, S., Houssaye, A., Nakajima, Y., Sander, P. M., 2017. A Triassic plesiosaurian skeleton and bone histology inform on evolution of a unique body plan. Science Advances 3, e1701144.

Wotzlaw, J.-F., Guex, J., Bartolini, A., Gallet, Y., Krystyn, L., McRoberts, C. A., Taylor, D., Schoene, B., Schaltegger, U., 2014. Towards accurate numerical calibration of the Late Triassic: High-precision U-Pb geochronology constraints on the duration of the Rhaetian. Geology 42, 571–574.

Xie, Y., 2014. Knitr: A comprehensive tool for reproducible research in R. In: Stodden, V., Leisch, F., Peng, R. D. (Eds.), Implementing reproducible computational research. Chapman; Hall/CRC.

Xie, Y., 2015. Dynamic documents with R and knitr, 2nd edn.. Chapman; Hall/CRC, Boca Raton, Florida.

Xie, Y., 2018. Knitr: A general-purpose package for dynamic report generation in R., https://cran.r-project.org/web/packages/knitr/.

Yager, J. A., West, A. J., Corsetti, F. A., Berelson, W. M., Rollins, N. E., Rosas, S., Bottjer, D. J., 2017. Duration of and decoupling between carbon isotope excursions during the end-Triassic mass extinction and Central Atlantic Magmatic Province emplacement. Earth and Planetary Science Letters 1, 1–10.

Zajzon, N., Kristály, F., Pálfy, J., Németh, T., 2012. Detailed clay mineralogy of the Triassic-Jurassic boundary section at Kendlbachgraben (Northern Calcareous Alps, Austria). Clay Minerals 47, 177–189.

Manuscript received: August 08, 2018
Revisions required: October 24, 2018
Revised version received: December 12, 2018
Manuscript accepted: December 12, 2018

Appendix 1

Taxalist Bonenburg

Spores

Conbaculatisporites mesozoicus Klaus 1960
Deltoidospora spp. Miner 1935
Densosporites fissus (Reinhardt 1964) Schulz 1967
Limbosporites lundbladii Nilsson 1958
Lycopodiacidites rhaeticus Schulz 1967
Perinosporites thuringiacus Schulz 1962
Polycingulatisporites spp. (Simoncsics & Kedves 1961) Morbey 1975
Polypodiisporites polymicroforatus (Orlowska-Zwolinska 1966) Lund 1977
Semiretisporis spp. Reinhardt 1962
Triancoraesporites reticulatus Schulz 1962

Pollen

Cerebropollenites thiergartii Schulz 1967
Enzonalasporites vigens (Leschik 1955) Schulz 1967
Granuloperculatipollis rudis (Venkatachala & Góczán 1964) Scheuring 1978
Lunatisporites rhaeticus (Schulz 1967) Warrington 1974
Perinopollenites elatoides Couper 1958
Pinuspollenites minimus (Couper 1958) Kemp 1970
Rhaetipollis germanicus Schulz 1967
Ricciisporites tuberculatus Lundblad 1954

Dinoflagellates

Dapcodinium priscum (Evitt 1961) Below 1987
Rhaetogonyaulax rhaetica (Sarjeant 1963) Loeblich & Loeblich 1968
Suessia swabiana (Morbey 1975) Below 1987

Appendix 2

The following appendix is available under https://doi.org/10.5281/zenodo.2536746
The repository contains the R Markdown file required to reproduce the paper as well as the palynological and geochemical data sets.